Cold fusion

V. A. Tsarev

P. N. Lebedev Physics Institute of the Academy of Sciences of the USSR
Usp. Fiz. Nauk **160**, 1–53 (November 1990)

The experimental and theoretical investigations of cold fusion, performed during the year after the discovery of this phenomenon, are reviewed. The results, obtained by different groups, concerning the detection of neutrons, γ-rays, and charged products of the reactions as well as analysis for the content of tritium and helium and calorimetric analysis are summarized. Information about experiments on the fracture of substances containing deuterium is presented. Different attempts to understand the mechanism of this phenomenon are discussed. An example of a substantially nonequilibrium mechanism, connected with the acceleration of ions in strong local electric fields, generated when hydrides fracture, is studied.

INTRODUCTION

The phenomenon of "cold fusion" or "low-temperature fusion" is unusual not only by its physical nature but also with regard to the unordinary and, to a certain extent, scandalous situation that has unfolded around it. The behavior of the "discoverers" Fleischmann and Pons undoubtedly played a fatal role in the story of cold fusion. Declining to perform detailed control experiments and bypassing the accepted procedure for discussing scientific results they immediately reported in the media their discovery of a simple, cheap, and ecologically clean method for producing energy by means of nuclear fusion. [We recall that Fleischmann and Pons reported on their work at a press conference on March 23, 1989 at Utah State University (USA). Approximately one week later S. E. Jones of Brigham Young University, also in the state of Utah, reported that his group had also discovered cold fusion independently.[1,2]] The general public and the business community, who usually trust scientific reports, were extremely excited and enthusiastic about the discovery of promising solutions to the energy problem confronting mankind. Hundreds of scientific groups all over the world tried to repeat the experiments of Fleischmann and Pons. The apparent simplicity of the experiments and their enormous potential significance attracted to this problem many people who previously had not thought about fusion. What the newspapers afterwards dubbed the "worldwide race for cold fusion" started. In the course of this race many investigations were performed hurriedly, without taking the necessary care, and the results, which were not properly checked, were immediately announced on the radio and television, in the newspapers, etc. Many serious investigators were, naturally, disgusted by all this. Belief in the reality of "fusion in a test tube" changed almost daily, depending on new reports from different laboratories in the world. The universal confusion during the first two to three months was aggravated by the virtually complete lack of scientific publications, which were replaced by teletype reports, telephone conversations, letters, rumors, etc. (a more detailed account of this dramatic period of research on cold fusion is given, for example, in Refs. 1–4).

By fall 1989, i.e., approximately six months after the first reports, the situation started to change. The uproar surrounding cold fusion quieted down significantly. Many publications finally started to appear in scientific journals, and concurrently the true state of affairs with regard to cold fusion started to become more apparent. By the end of 1989 the literature on the experimental and theoretical aspects of cold fusion already was so extensive that it was apparent that a review of the research performed during the previous year was in order. Reviewing the work on cold fusion at this stage is unquestionably a very unpleasant problem, first, because the experimental situation is still unsettled and there are significant quantitative and qualitative uncertainties and, second, because there is no generally accepted point of view regarding the mechanism of cold fusion.

However considerations of a different sort can be presented. A "change of regime" is now occurring in cold-fusion research. After widespread disillusionment and pessimism replaced the initial uproar and uncontrollable excitement, interest in cold fusion is now reviving, but it is now channeled in the direction of calm and professional scientific investigations. The period of quick and simple experiments is being replaced by a period of painstaking and careful investigations. For this reason, it may now be useful to examine the "initial conditions" for this new stage, to summarize what is now known about cold fusion. This pertains not only to experiments, but also to theory, where it has been found that many initial directions in the search for the mechanism of cold fusion are dead ends, while other directions, which could still be successful, require further and more detailed investigation and comparison with experiment.

Another reason for discussing different aspects of research on cold fusion is that the problem is a multilevel, interdisciplinary one that includes questions in electro- and radiochemistry, the chemistry of solids, thermodynamics, metallurgy, the physics of hydrogen-induced fracture of metals, and nuclear physics.

It has been estimated that about 100 experimental investigations and approximately the same number of theoretical papers on cold fusion have now been published. Unfortunately, by no means all of these works were available to me at the time this review was written (January 1990). For this reason, I apologize at the outset to those authors whose works are not reflected in this review. But it is quite obvious that the "massive" character of the research and the continuous publication of new papers concerning the most diverse directions make a comprehensive review of all the investigations of cold fusion quite unrealistic. However, even the publications that will be studied in this review give a quite complete idea of the status of research on cold fusion. This review is organized as follows.

Experiments on cold fusion are reviewed in Sec. 1. First, the basic information about the work performed by Fleisch-

 0038-5670/90/110881-30$01.00

mann and Pons[5] and by Jones' group[6] is reviewed. Next, the results reported by different groups concerning the detection of neutrons, γ-rays, and the charged products of cold-fusion reactions as well as an analysis of the electrodes and the electrolyte for the content of tritium, ^{3}He, and ^{4}He, and finally calorimetric measurements are summarized. Information about experiments in which mechanical damage to deuterium-containing materials together with neutron emission were recorded is also presented. Although these investigations fall somewhat outside the mainstream of experiments in which cold fusion was investigated under conditions of saturation of transition metals with deuterium, they are, apparently, closely related. It is shown in Sec. 4 that there is some basis for believing[7,8] that the processes occurring when metals are saturated with deuterium are based on the same mechanism as in the case when ionic single crystals containing deuterium fracture. In this sense the work reported by V. A. Klyuev *et al.*,[9] who were the first to observe neutron emission accompanying mechanical fracture of LiD single crystals, can be regarded as the first experimental observation of the phenomenon of cold fusion. In concluding this section, conclusions are drawn regarding the present status of cold-fusion experiments.

In Sec. 2 some information about metal-hydrogen systems is presented. This information could be useful in the theoretical discussion of cold fusion. The structure and bonds in these systems, the transfer of hydrogen and its isotopes in metals, the formation of hydrides, and fracture accompanying hydrogen absorption are examined.

Section 3 is devoted to a discussion of different attempts to understand the mechanism of cold fusion. The fusion of colliding nuclei and nuclei bound in a molecule are studied. The degree of "compression" required to achieve fusion at the level observed in some experiments is estimated. The results of calculations of the possible screening of the Coulomb barrier in metals are discussed. Models with a "heavy electron," catalysis by cosmic muons and hypothetical heavy particles, and a number of other models are examined. Some effects that can produce spurious signals in cold-fusion experiments are also discussed. The main conclusion of this section is that cold fusion cannot be satisfactorily explained based on the traditional ideas of nuclear physics and the physics of solids under equilibrium conditions.

An example of a substantially nonuniform "acceleration" mechanism, which, apparently, is the basis for the currently most promising model of cold fusion, is studied in Sec. 4. It should be noted that in application to electrons the idea of acceleration in the strong electric fields that are generated by mechanical fracture of ionic crystals and adhesion layers was first formulated based on a study of the phenomenon of mechanoemission (see, for example, Refs. 10 and 11). Later it was suggested that exoenergetic nuclear reactions can occur in these fields and the above-mentioned experiment on the mechanical fracture of LiD single crystals, confirming this proposition, was performed.[9] The next nontrivial step was taken in Refs. 7 and 8, where it was asserted that the acceleration mechanism could operate in cold-fusion experiments under conditions when transition metals are saturated with deuterium and justification for this assertion was provided. In Sec. 4 a possible scenario of cold fusion is described, the conditions required for the "acceleration" mechanism to be realized in the hydrides of transition metals (Pd, Ti, ...) are discussed, and the efficiency of this mechanism is estimated. An experimental program designed to check the basic assumptions and consequences of the acceleration model is discussed in the last section.

In completing this introductory part, in order to facilitate further references we present in Table I a list of fusion reactions of light nuclei that will be studied in this review in connection with experiments on cold fusion. Reactions involving Li are possible when an electrolyte containing LiOD is employed. The numbers in the third column indicate the energy released (in MeV) and the numbers in parentheses denote the energy carried away by the final products. The last column gives the number of fusion reactions of each type occurring per second and generating 1 W of power (1 MeV $= 1.602 \cdot 10^{-12}$ J).

As one can see from Table I, all reactions are exothermal. They do not have thresholds and, generally speaking, they can occur at arbitrarily low relative energies. However, the probabilities of these reactions (or the "reaction rates") will be very low.

1. EXPERIMENTAL INVESTIGATIONS OF COLD FUSION

1.1. The investigations of Fleischmann and Pons[5] and of Jones' group[6]

The pioneering publications of these two groups are undoubtedly quite well known to anyone interested in the problem of cold fusion. Nonetheless, in order to give a complete presentation as well as for further reference, it is useful to review the basic information concerning these experiments.

1.1.1. In Ref. 5 electrolytic saturation of the cathode with deuterium was performed in a 0.1 mole/liter solution of LiOD in the mixture 99.5% D_2O + 0.5% H_2O. The electrodes consisted of Pd, in the form of foil, rods, and cubes. The current density j in different experiments ranged over wide limits from 0.8 mA·cm^{-2} to 512 mA·cm^{-2}.

TABLE I.

Reaction		Energy release, MeV	Number of reactions in 10^{12} s^{-1} per watt
p+D → ^{3}He+γ (5,5)	(1B)	5,5	1,1
D+D → ^{3}He (0,82)+n (2,45)	(2B)	3,27	1,9
D+D → T (1,01)+p (3,02)	(3B)	4,03	1,6
D+D → ^{4}He+γ (23,8)	(4B)	23,8	0,26
D+T → ^{4}He (3,5)+n (14,1)	(5B)	17,6	0,36
D+^{6}Li → ^{4}He+^{4}He	(6B)	22,4	0,28
D+^{6}Li → ^{7}Li+p	(7B)	5,0	1,3
D+^{6}Li → ^{7}Be+n	(8B)	3,4	1,8
D+^{7}Li → ^{4}He+^{4}He+n	(9B)	15,1	0,41

The thermal balance was measured both at low (0.8–1.6 $mA \cdot cm^{-2}$) and high (up to 512 $mA \cdot cm^{-2}$) current density in a Dewar flask, placed in a reservoir of water, whose temperature was maintained at 300 K. The temperature in the cell and the reservoir was monitored with thermometers. The solution was mixed as necessary.

The spectrum of γ-rays, thought to be produced in a reaction in which the neutrons formed in the process (2B) are captured

$$n+p \rightarrow D+\gamma \ (2{,}22) \qquad (1.1)$$

was recorded with a NaI scintillation detector. The correction for the background was made by subtracting out the spectrum measured above an identical water reservoir placed ten meters away from the working cell.

The neutron flux was measured with a standard dosimeter based on BF_3 counters. The efficiency of the dosimeter with respect to 2.5 MeV neutrons was equal to $\varepsilon_n \approx 2.4 \cdot 10^{-6}$ (this estimate includes the geometric factor). The neutron background was measured 50 m from the working cell. The measurements were performed in a basement and usually lasted for 50 h.

In addition, the rate of generation and accumulation of tritium, presumably via the channel (3B), was measured. For this, 1 ml samples of the electrolyte were extracted every two days and their β activity was determined.

The following results were presented:

1) Heat in excess of the supplied electric energy was observed. In a number of cases this excess heat exceeded by several times the energy supplied, and on the average it was of the order of ≈ 10 W per cm^3 of Pd and could be maintained for a period of $\sim 10^2$ h, during which time up to ~ 4 $mJ \cdot cm^{-3}$ of energy was released.

2) Gamma rays, with the spectrum shown in Fig. 1, were recorded. In the opinion of the authors this confirmed that these γ-rays were produced as a result of neutron capture.

3) The dosimeter showed the presence of a neutron flux, whose intensity is in agreement with the intensity of the γ-rays and is equal to $\dot{N}_n \approx 4 \cdot 10^4$ sec^{-1} (approximately three times higher than the background).

4) The accumulation of tritium in the electrolyte shows that the reactions (3B), whose rate is $\dot{N}_T \approx (1\text{–}2) \cdot 10^4$ sec^{-1}, comparable to $\dot{N}_n$, occur.

Since a rate $\sim 10^{11}$–10^{14} s^{-1}, substantially higher than

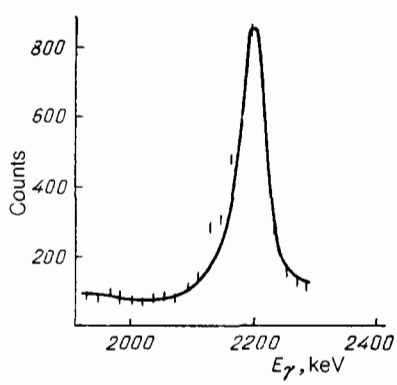

FIG. 1. Shape of γ-ray line given in Ref. 5

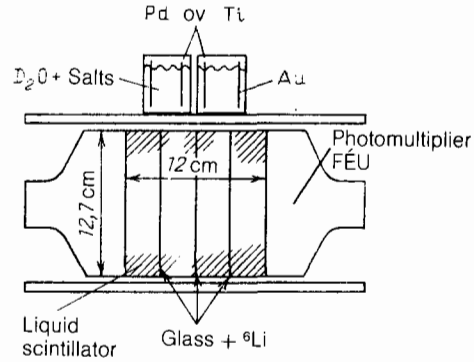

FIG. 2. Diagram of the apparatus used in Ref. 6.

follows from N_n, is required in order to explain the calorimetric measurements in terms of nuclear fusion (2B) the authors conclude that in their electrolytic cell energy is released primarily as a result of some other, unknown nuclear processes.

1.1.2. The arrangement of the experiment of Jones et al.[6] is shown in Fig. 2. The neutron spectrometer consists of a liquid organic scintillator (BC-505), contained in a glass cylinder, into which three scintillating glass plates with added ^{6}Li were placed. The neutrons lose energy in the liquid scintillator as a result of repeated collisions, and the light generated in the process gives information about the energy of the neutrons. After moderation, the reaction $n + {}^6Li \rightarrow T + {}^4He$, which causes scintillation in the glass, occurs. Photomultipliers record two characteristic signals, and the coincidence of these signals with a delay of 20 μs is identified as a neutron.

Background measurements, in which D_2O was replaced in the cells by H_2O, were performed or the measurements were performed with D_2O but with no current. In all background measurements there was no peak in the region of 2.5 MeV, and the background counting rate in this region was equal to 10^{-3} s^{-1}.

Jones *et al.* employed an electrolyte with a very complicated composition and cathodes made of Ti and Pd. The cathodes had different shapes and their mass ranged from 0.05 to ≈ 5 g. From four to eight cells with 20 ml of electrolyte ($U = 3$–25 V, $j = 10$–500 mA) operated simultaneously.

Figure 3 shows the results of the measurements of the neutron spectrum, accumulated over 14 series and presented in the form of the difference between the indications of the

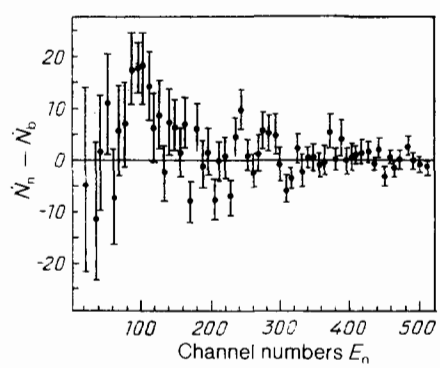

FIG. 3. Neutron spectrum after the background is subtracted out.[6]

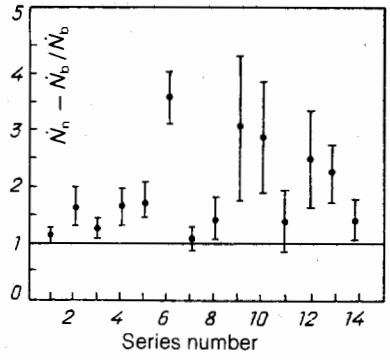

FIG. 4. Signal-to-background ratio in different series.[6]

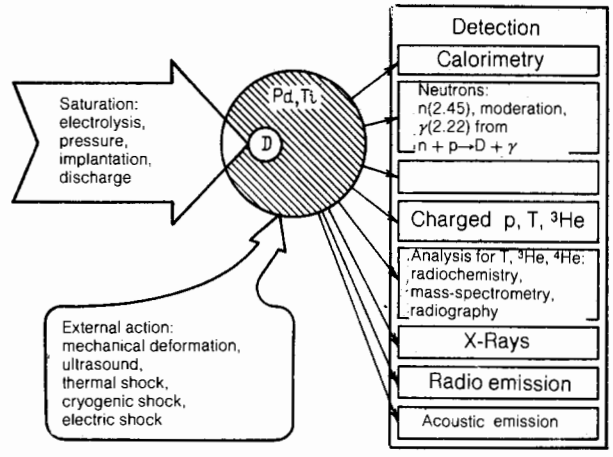

FIG. 5. General scheme of cold-fusion experiments.

detector with the working cell and the background counts. A characteristic structure in the form of a peak centered on the channel 100, corresponding to an energy of ≈ 2.5 MeV, can be seen. Figure 4 shows the results of each series of measurements separately in the form of the ratio of the signal due to 2.5 MeV neutrons to the background in the same series. The series 6, in which the signal is quite sharp, is especially interesting. In this series the neutron counting rate increased approximately 1 h after the start of electrolysis and dropped to the background level after 8 h.

A convenient characteristic of the intensity of the reactions is the counting rate per pair of deuterium nuclei:

$$\Lambda = \frac{\dot{N}_n}{\varepsilon_n N_{DD}},$$

where $\dot{N}_n$ is the neutron counting rate in the detector, which in series No. 6 was equal to $(4.1 \pm 0.8) \cdot 10^{-3}$ s^{-1} in the region of 2.5 MeV; $\varepsilon_n = 1.0 \pm 0.3\%$ is the efficiency of the detector (including the geometric efficiency); and, $N_{DD} \approx 4 \cdot 10^{22}$ is the number of DD pairs in an electrode having a mass of 3 g. Thus in the series No. 6 Jones *et al.* found for the rate of cold fusion

$$\Lambda \approx 10^{-23} \text{ s}^{-1} (\text{DD})^{-1}. \quad (1.2)$$

If, however, the average counting rate for all series is used to determine Λ, then we obtain a figure that is approximately seven times lower than (1.2). We shall call the rate of fusion $\Lambda \approx 10^{-24}$–10^{-23} s^{-1} (DD)$^{-1}$ the Jones level. The corresponding neutron-emission intensities of a Ti source saturated to the composition TiD_2 are equal to $N(TiD_2) \approx 10^{-2}$–10^{-1} s^{-1}g^{-1}.

In Sec. 1 below we shall discuss the experiments that were performed by different groups right after Refs. 5 and 6 appeared and whose purpose was to check the results of Refs. 5 and 6 and to investigate further the phenomenon of cold fusion.

1.2. General arrangement of cold-fusion experiments

In most experiments on cold fusion the metals were saturated with deuterium by means of electrolysis or from the gas phase under pressure. In some cases ion implantation or a gas discharge was employed. The transition metals Pd and Ti, which have a high capacity for dissolving hydrogen and its isotopes, are, as a rule, used as the deuterium "accumulator." In some experiments other metals (Zr, V, ...) or alloys (Pd–Ag, Ti–Al, Pd–Ag–Au, ...) were also used.

The general arrangement of an experiment in which a search is made for different manifestations of nuclear reactions is shown in Fig. 5. The experiments can include calorimetry, the detection of neutrons, γ-rays, and charged particles, radiochemical methods for detecting tritium, mass spectrometric methods of searching for ^{3}He and ^{4}He, and, finally, the detection of the x-rays which are produced as a result of the excitation of atoms of the metal and which, in the general case, should accompany any nuclear reactions occurring in a condensed medium.

In addition, under a special assumption about the acceleration mechanism of cold fusion (see Sec. 4), electromagnetic and acoustic radiation sensors as well as various means by which one can try to affect the flow of cold-fusion processes (mechanical action, ultrasound, thermal, cryogenic, and electric shocks, etc.[7,8]) can be employed to record the associated phenomena.

Since the general interest in cold fusion stems primarily from the hope that it can be used to produce electricity, interest was directed initially toward calorimetric measurements. It is obvious, however, that such measurements make sense only if the heat effect is large. If it is assumed that the usual nuclear reactions (2B) and (3B) occur, then the neutron yield at the Jones level corresponds to power production levels ($\sim 10^{-12}$ W) that cannot be measured by direct calorimetric measurements. In addition, even if the excess heat released in cold fusion is quite large, the measurement of this excess heat is a very difficult and delicate problem, because the heat is released against the thermal background created by electrochemical processes.

The best signature of cold fusion is obviously the detection of neutrons (at least, under the assumption that fusion proceeds in the standard channels at low rates). According to the well-known properties of the cross sections of the processes (2B) and (3B) it is expected that when deuterium nuclei fuse 2.45-MeV neutrons are produced in approximately 50% of the events. Such neutrons easily pass through the material of the electrode, the electrolyte, and the cell walls, and they can be recorded by the detectors.

Gamma rays can be produced in cold-fusion experiments either as secondary products accompanying the capture of thermalized neutrons, produced in the reaction (2B) in the matter surrounding the cell (for example, in the coolant water, in the moderator, etc.) via the reaction (1.1) or as

primary products of fusion in the channels (1B) and (4B). The first of these reactions can occur in the presence of a random or specially introduced impurity either of ordinary water during electrolysis or hydrogen gas in the case of saturation from the gas phase and results in the emission of γ-rays with energy $E_\gamma \approx 5.5$ MeV. The rate of this reaction at very low energies of the fusing nuclei can be higher than the rate of the reactions (2B) and (3B) (see Sec. 3). In the case when the acceleration mechanism operates (i.e., under microscopically hot conditions), however, it proceeds more slowly than the reactions (2B) and (3B). As regards the reaction (4B), its probability is five to six orders of magnitude lower than that of the reactions (2B) and (3B). These remarks should be kept in mind when evaluating the experimental data on the detection of γ-rays.

It is extremely difficult to detect directly the charged particles produced as a result of cold fusion, since at the expected energies the ranges of p, T, and ^{3}He in the matter of the electrodes (Pd, Ti) or in the electrolyte (D_2O, H_2O) are very short. (Thus the ranges of T, ^{3}He, and p from the reactions (2B) and (3B) in Ti are, respectively, 2.5–3 μm and 75 μm.)

According to the exotic "Mössbauer" mechanism of fusion (see Sec. 3) it is possible that α particles with energy ≈ 23 MeV could be produced. In principle, such particles can also be detected by direct methods.

The formation of T, ^{3}He, and ^{4}He in cold-fusion processes can be studied by using samples of the electrode material or electrolyte and by performing radiochemical or mass-spectrometric measurements.

Finally, a common signature of any (including unknown) nuclear-fusion reactions should be the emission of x-rays, which are produced when the metal atoms are excited by the fast products of nuclear reactions. The drawback of this method, like also the methods of searching for T, ^{3}He, and ^{4}He, is that it is less sensitive that the neutron-detection method (see Secs. 1.6 and 1.7).

In Sec. 4 we shall discuss a hypothesis according to which the cold-fusion reactions are generated when deuterium ions are accelerated in the microcracks that are formed when metals are saturated with deuterium. This mechanism can be checked with the help of various coincidence experiments, in which the detection of the products of fusion (n, γ, p, ...) is correlated with the signals produced as a result of crack formation (electromagnetic radiation at different wavelengths and acoustic radiation). In addition, the acceleration model also indicates the possible mechanisms by which cold-fusion processes can be affected by the intensification of crack formation (mechanical strains, ultrasound, thermal, cryogenic, and electric shocks, etc.) and with which the detection of the products of cold fusion can also be correlated.[7,8]

The above-mentioned methods of searching for cold-fusion reactions differ with respect to the degree of complexity, sensitivity, information content, and the specific nature of the arrangement of the experiments. Different considerations (availability of apparatus, experience, etc.) can dictate in each specific case the choice of one or another channel of detection. It is obvious, however, that in order to make a comprehensive study of cold fusion and to determine its nature data must be accumulated in all possible channels.

The last remark concerns the problem of backgrounds. The first experiments on checking the results reported in Refs. 5 and 6 already showed that the cold-fusion signal, if it exists, is quite weak and in different channels it is close to the background level, determined by cosmic rays, decay of radioactive isotopes in the surrounding materials, etc. This means that the background must be carefully analyzed and suppressed as much as possible. Many sources of spurious effects have been indicated in a number of studies; some of them are studied below in Sec. 3. In later experiments, as a rule, the background was suppressed by some method. Figure 6 shows the typical schemes, including passive and active shielding. It was also found that it is best to use pure materials and low-background laboratories. Thus the Bologna[12] and Frascati[13] groups performed measurements in the Gran Sasso underground neutron laboratory ($h = 3500$ m water thickness equivalent), which made it possible to reduce the neutron background by a factor of $\sim 10^3$, and the γ-ray background by a factor of 50 below the values observed under typical laboratory conditions.

1.3. Experiments on neutron detection

We shall begin with the largest group of experiments in which neutron detection was performed. The following methods were employed:

a) Detection of fast neutrons based on recoil protons, as a rule, with the help of detectors based on liquid or solid scintillators (NE 102A, NE 213, stilbene, paraterphenyl, etc.). Gamma-ray or charged-particle pulses (primarily cosmic-ray muons) were discriminated with the help of a method based on an analysis of the pulse shape and taking into

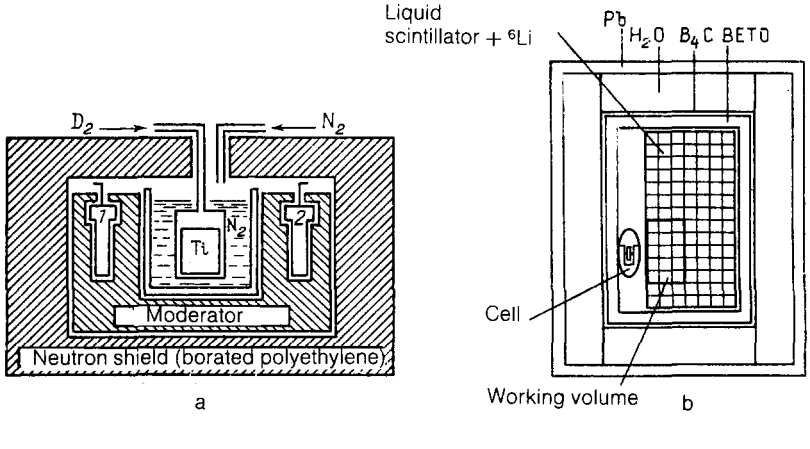

FIG. 6. Examples of apparatus with passive (a) (Ref. 36) (1, 2 are neutron detectors) and active (b) (Ref. 40) shielding.

account the fact that neutrons give a larger pulse width than do γ-rays and muons. In addition, in Ref. 14 dielectric track detectors were employed to detect recoil protons.

b) Detection of neutrons, moderated to thermal energies with the help of hydrogen-containing moderators (water, paraffin, polyethylene), with the help of counters based on BF_3, ^3He, etc.

c) In a number of investigations both methods are employed and the time delay, which typically is equal to 10 μsec and is determined by the moderation process, was taken into account.

d) Detection of γ-rays produced when neutrons are captured in the material surrounding the cell.

To simplify the discussion we shall divide the experiments in which neutrons are detected into four groups. The first group (see Sec. 1.3.1) consists of investigations in which the emission of tens and hundreds of neutrons in groups over short time intervals (from hundreds of μsec to several minutes)—so-called neutron bursts—was observed. The second group (see Sec. 1.3.2) consists of experiments in which neutron emission, on the average, approximately at the Jones level or somewhat higher was detected over a long period of time (hours), but correlations in time either were not investigated or were not observed. The third group (see Sec. 1.3.3) consists of studies in which no statistically significant above-background neutron signal was found. The accuracies of the experiments were sufficient to exclude the effect at the Fleischmann-Pons level, but they do not permit checking the effect at the Jones level. If this last level is assumed to be the characteristic level, to be checked, then the studies in this group do not make it possible to draw definite conclusions. Finally, in the investigations comprising the fourth group (see Sec. 1.3.4) a statistically significant signal also was not observed, but the accuracy of the measurements

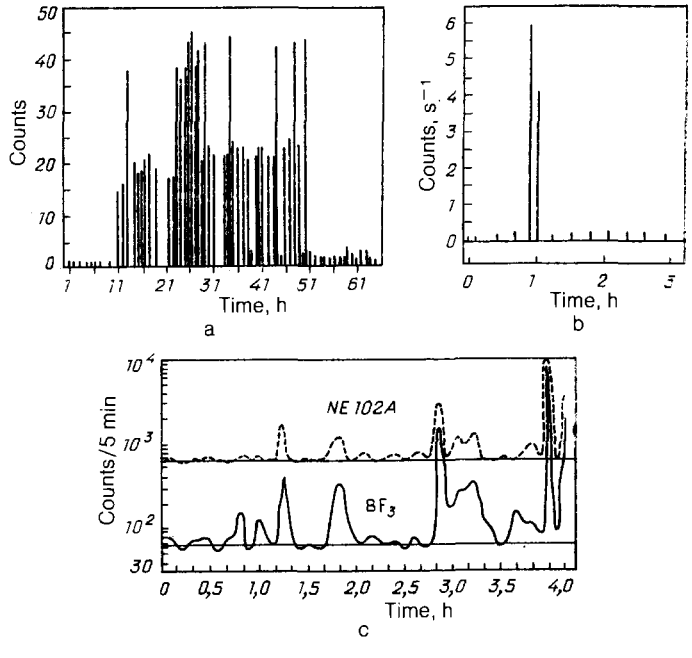

FIG. 7. Neutron bursts. a) Ref. 15, b) Ref. 16, c) Ref. 17, d, e) Ref. 13.

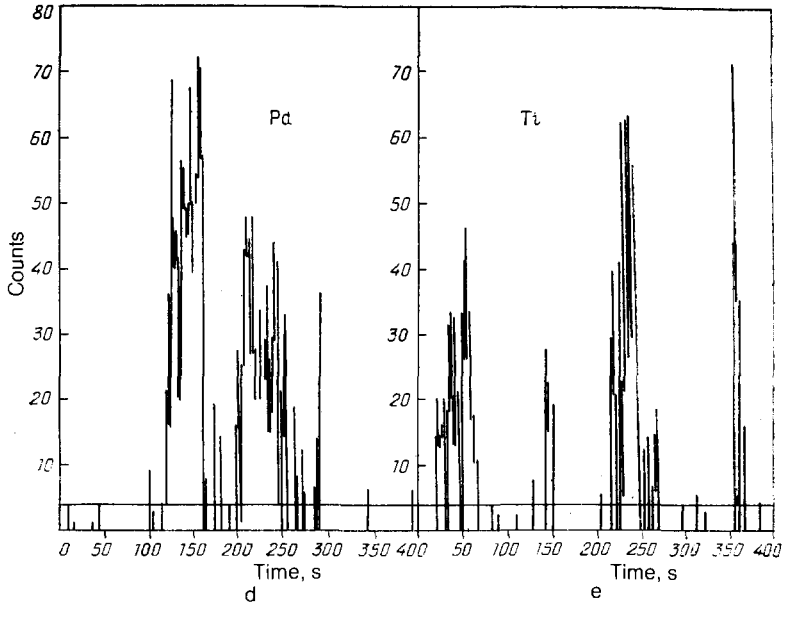

TABLE II.

Reference	Metal	Method of saturation	Detectors	Background in the detector	Signal in the active period	
					Counter	Source, $s^{-1}\cdot g^{-1}$
[3]	Ti, Pd	Electrolysis	^{3}He, plexiglass + ZnS(Ag)	—	10^3	$(\Lambda\approx 10^{-22}\,s^{-1}\,(DD)^{-1})$
[15]	Ti	D_2, 50 atm, 77—300 K	BF_3, $\epsilon\approx 5\cdot 10^{-5}$	$6{,}4\cdot 10^{-4}\ s^{-1}$	2800/40 h	4
[16]	Ti, Pd	D_2, 40 atm, 77—300 K	18×(^{3}He), $\epsilon\approx 34\%$	$5\cdot 10^{-3}\ s^{-1}$	180/128 μs	$8\cdot 10^3$
[17]	Pd(Ag), Ti	Electrolysis	Bank of BF_3	65/300 s	26 000/300 s	$7{,}5\cdot 10^4$
		D_2, 50 atm	NE 102A, 24×(^{3}He), $\epsilon\approx 10\%$	650/300 s	3900/40 s	$2\cdot 10^3$
[13]	Pd, Ti(Al)	Electrolysis	NaI (Tl), $\epsilon\approx 1\%$	$10^{-6}\ см^{-2}\,s^{-1}$	$(1—2)\cdot 10^3/0{,}6$ s	$5\cdot 10^3$
			^{3}He	$<1\ s^{-1}$	4100/205 s	$0{,}75\cdot 10^3$
			Plastic	$<1\ s^{-1}$		

makes it possible to set an upper limit on the rate of fusion that is significantly lower than the Jones level.

1.3.1. Observation of neutron bursts. Neutron bursts were observed in Refs. 3, 13, and 15–17 with both electrolytic and gas saturation of Pd, Ti, and some alloys.[1)] Thermal cycling was employed in the experiments with gas. Thus in Ref. 16 Ti in the form of shavings, granules, etc. was placed in a steel cylinder. The cylinder was filled with deuterium up to a pressure of $\approx$40 atm and then submerged for some time in liquid nitrogen. As the liquid nitrogen evaporated the temperature rose from 77 to 300 K. Then liquid nitrogen was once again poured into the Dewar flask, and the thermal cycle was repeated. Neutron activity was observed in the cylinders after several thermal cycles, as a rule, during heating up to the temperature -30 °C (approximately one hour after the cycle starts). In general, the appearance of activity soon after the start of the experiments (tens of minutes or hours) is characteristic for all experiments in this group. The sharpest results are presented in Fig. 7, and the basic information about these experiments is given in Table II.

1.3.2. Uncorrelated emission of neutrons. In Refs. 12, 14, and 18–26 (see Table III) the neutron fluxes averaged over significant time intervals (typically tens of hours) were measured. No correlation was observed in narrow time intervals or it was not investigated. We note that uncorrelated emission was also observed in some publications in the first group. Thus in Ref. 16, in one series of measurements over a period of 12 h, the total number of detected neutrons exceeded the background level by 11σ. The results of these measurements are presented in Fig. 8 (the experimental dots correspond to averaging over time intervals of $\approx 10^4$ s). Table III gives the basic information about experiments from the second group. We note that it is often difficult to make a quantitative comparison of the results obtained in different studies. On the one hand, the experimental conditions can often differ significantly, while on the other, because the mechanism of cold fusion is not known, it is not clear how best to present the results—for 1 g of the metal, 1 cm^3 of volume, or per unit surface area. Also the degree of deuterium saturation of the metal (i.e., the ratio D/Me) is often unknown. For consistency we shall present the results for 1 g of the electrode material, though in reality such a scaling may not be adequate, if the process is significantly of a surface character. At the same time, it is difficult to scale to the unit surface area of the metal, since material in the form of

TABLE III.

Reference	Metal	Method of saturation	Detectors	Results
[3]	Pd, Ti	Electrolysis	^{3}He, Plexiglas + ZnS(Ag)	$N_r/N_b\approx 3-5$, $\Lambda\approx 10^{-22}\,s^{-1}\,(DD)^{-1}$
[19]	Pd		Paraterphenyl LiI(Eu), LiF (TiO_2)	$10-100 s^{-1}$
[16]	Ti	D_2, 40 atm	^{3}He	Signal stronger than the background by 11σ
[12]	Ti	Electrolysis	NE 213 $\epsilon\approx 4\cdot 10^{-2}$, $\gamma/n\sim 10^{-4}$	$875\pm 183\ h^{-1}\,(3\ g)^{-1}$
[20]	Pd		BF_3, $\epsilon\approx 1{,}45\cdot 10^{-5}$	$50\pm 23\ s^{-1}$ average over 8 h
[21]	Pd		BF_3, plastic, stilbene, NaI(Tl)	$0{,}1\ s^{-1}$
[22]	Pd		NE 213, γ/n	$10^2\ s^{-1}$
[23]	Pd		—	Signal several times stronger than the background
[24]	Pd		NE 213, γ/n	$\Lambda\approx 10^{-23}\,s^{-1}\,(DD)^{-1}$ average over 18 days
[25]	Pd		—	Signal 3 to 4 times stronger than the background; the active period is 2 h
[14]	Pd–Ag–Au		Dielectric track detector	$8\pm 4\ s^{-1}$
[26]	Pd,	Ion implantation	SNM-5	$10^2\ s^{-1}$

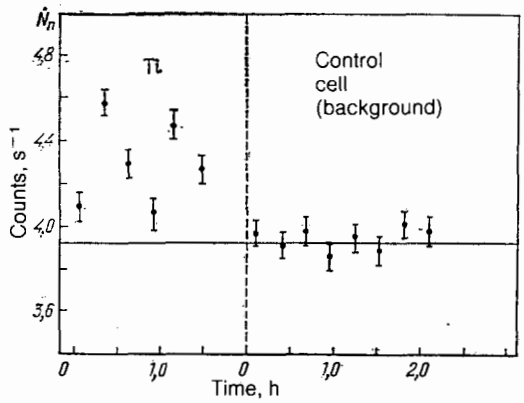

FIG. 8. Uncorrelated neutron emission.[16]

shavings, granules, spongy tablets, etc. is often used. We also note that information about some investigations is obtained from abstracts, the information in which is very incomplete.

As an example, we shall discuss the results of Ref. 26, where interesting information was obtained about the dependence of the intensity of cold-fusion processes on the experimental conditions. To saturate the metal with deuterium the metal sample (thin palladium films, $\delta = 0.15$–$0.6\,\mu$m, or titanium foil, $\delta = 0.3$ mm) was irradiated with a monoenergetic beam of 25-keV D_2^+ ions with current density 30–40 $\mu A \cdot cm^{-1}$. The neutrons were detected with SNM-5 slow-neutron detectors containing boron, a paraffin moderator, and a cadmium screen (the efficiency $\varepsilon_n \approx 2 \cdot 10^{-4}$ pulses/neutron). The main results were obtained in experiments in which, after being saturated with deuterium, the Pd and Ti samples were heated from 77 to 1300 K at rates of 1.5–3 K/s. The results of the measurements, in the form of the ratio of the neutron-detector signal $\dot{N}$ to the average background $\dot{N}_b$ ($\approx 2 \cdot 10^{-2}$ pulses/s), are shown in Fig. 9 as a function of the temperature of the sample. For both metals two temperature ranges in which the signal exceeded the background were observed: 100–400 and 900–1300 K in the case of Pd and 100–300 and 600–1200 K in the case of Ti. Comparing the curves of N/N_b shown in Fig. 9 with the curves of desorption of the implanted deuterium, presented in Fig. 10, shows that the two sets of curves are definitely correlated. The authors point out that the counting rate of the neutron detector was also observed to exceed the background level under the following circumstances:

—when the Ti samples are repeatedly heated from 77 K up to temperatures above 1300 K and

—when both Ti and Pd are cooled from the irradiation temperatures (≈ 100 K) to 77 K after irradiation is stopped.

In Fig. 9 the maximum average counting rates of the detector with respect to the background level are equal to 2...2.3, which, taking into account N_b and the efficiency ε_n, corresponds to a neutron source with intensity $\approx 10^2$ neutrons/s.

It is important to emphasize that neutron emission was observed only when the samples were heated or cooled, i.e., it is associated with a nonequilibrium state of the metal-deuterium system.

Another important feature of Ref. 26 is that in it the yield of all products of DD fusion in the channels (2B) and (3B) (see Sec. 1.5) was recorded for the first time within the same experiment and it is shown that the energies of the charged particles correspond to their expected values (although the yield of charged particles is more than an order of magnitude lower than the neutron yield).

We note that all papers on neutron detection which we studied employ, as a rule, electronic methods. Reference 14 is an exception. In Ref. 14 dielectric track detectors (DTDs) were employed to detect neutrons based on the recoil protons. Analogous detectors were also employed in Ref. 27 in order to detect fast α particles (see Sec. 1.5). The DTD method has a number of interesting features, to which it is useful to call attention in connection with experiments on cold fusion. Dielectric track detectors have the following characteristic features:[14] There exists a detection threshold, spatial correlation of events in the presence of a strong background due to weakly ionizing particles can be revealed, there is no delay, information is stored for a long time, there are no communication lines, the detectors can be placed in locations that are difficult to reach, the detectors are resistant to radiation, the geometric factor is relatively high, and, finally, a good record is obtained and even single events are detected with great reliability.

1.3.3. Experiments with low sensitivity.. Information about experiments[28,35] in which cold fusion was not observed but the sensitivity made it impossible to check the effect at the Jones level is presented in Table IV.

1.3.4. Experiments with negative results. In a number of highly accurate experiments,[27,36–40] a neutron signal due to cold fusion was not observed. The errors in the measurements were significantly smaller than in experiments from the third group, and this made it possible to set an upper limit on the rate of cold fusion at less than the Jones level. The characteristics of these experiments are presented in Table V. There arises the question of how the negative results obtained in the investigations in the fourth group should be interpreted. The explanation of these results could be connected with the sporadic, nonreproducible character of cold fusion, which is especially obvious in experiments from the first group. It is important to note the following typical feature of experiments from the fourth group. In striving to pack as much deuterium as possible into the volume of the metal, in these studies, as a rule, prolonged "charging" is performed and measurements are made only after the charg-

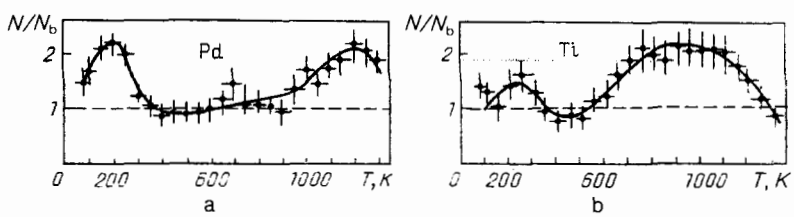

FIG. 9. $(N/N_b)_{av}$ as a function of the temperature for Pd (a) and Ti (b).[26]

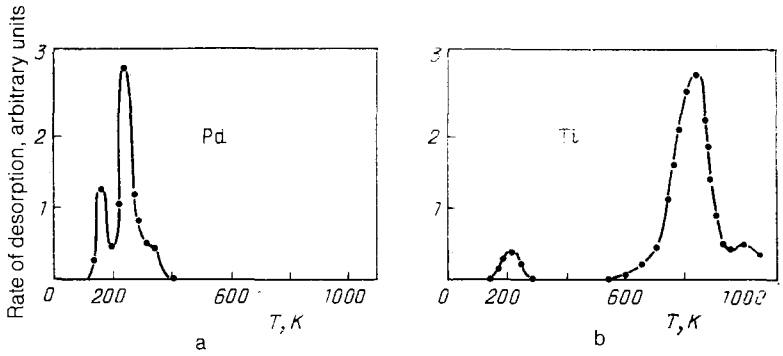

FIG. 10. Spectra of thermal desorption of D_2 from Pd (a) and Ti (b).[26]

ing is completed. Reference 37, for example, is typical in this respect. In Ref. 37 the charging was performed, as a rule, over a period of hundreds of hours (a 24-h charging period was employed in only one series of experiments). At the same time, as pointed out in the discussion of the studies belonging to the first group, the appearance of cold-fusion signals in fresh samples soon after the onset of saturation is a characteristic feature of these experiments. Based on the theoretical considerations presented in Sec. 4, it can be conjectured that in the experiments belonging to the first group the moment at which the cell was in the "active state" was simply missed.

1.4. Gamma rays

In a number of experiments 2.2, 5.5, and 23.8 MeV γ-rays, which can arise as primary or secondary products of nuclear fusion in the processes (1.1), (1B), and (4B), were detected in order to search for cold fusion.

As we have already noted above, the first of these reactions occurs when thermalized neutrons are captured, i.e., it actually indicates that such neutrons were emitted. The efficiency of this method of neutron detection is determined by the capture cross section, the properties of the materials surrounding the cell, and the efficiency of the γ-ray detector, and it is usually equal to $\sim 10^{-4}$, i.e., lower than the efficiency of typical neutron detectors. The second reaction in cold-fusion experiments can occur if H_2O or H_2 is present as an impurity in the cell. The rate of this reaction, relative to the channels (2B) and (3B), depends on the character of the processes: for cold fusion it is higher and for hot fusion it is lower than for (2B) and (3B) (see Sec. 3). The last reaction is suppressed relative to the channels (2B) and (3B) by five to six orders of magnitude.

As a rule, NaI, BGO, and Ge crystal detectors are employed to detect γ-rays.

We recall that the detection of the 2.2 MeV γ-ray line was presented already in the first paper (Ref. 5) as one proof of the discovery of cold fusion. Later, however, these results on γ (2.2 MeV) were criticized, and Fleischmann and Pons were ultimately forced to reject them at the Los Angeles conference. The discussion in this connection[28,41-43] is quite instructive, and therefore we shall briefly recall the basic arguments of the opponents.

a) The line width, presented by Fleischmann and Pons, is at least two times smaller than the line width admitted by the resolution of their apparatus. The MIT group[41,43] employed a Pu/Be neutron source, in which α particles from $^{239}_{94}$Pu generate neutrons via the reaction (α, n) on Be. The source was calibrated with an accuracy of 10% and gave $1.5 \cdot 10^6$ neutrons/s. It was placed in a tank containing water; the geometry was analogous to that employed in the experiment of Ref. 5. The neutrons from the source were thermalized in the water, and γ-rays produced when neutrons are captured were observed with the help of a NaI spectrometer similar to that employed in Ref. 5. The measured resolution at 2.22 MeV was equal to 5%, instead of the 2.5% claimed by Fleischmann and Pons.

b) The plot of the γ-ray line presented in Ref. 5 (see Fig. 1) does not contain the distinct characteristic of a γ-ray spectrum—the so-called Compton edge at 1.99 MeV.

c) The estimate given in Ref. 5 of the neutron yield based on the intensity of the γ-ray signal is approximately 50 times higher than the result obtained by direct neutron

TABLE IV.

Reference	Metal	Method of saturation	Detectors	Result
[28]	Pd	Electrolysis	Li (Eu) I-Dosimeter	Upper limit not indicated
[29]	Same		NE 213	$<1\ s^{-1}$
			$\epsilon = 0.025 \pm 0.008$	(average over 5 days)
[30]			Plastic	$<1 - 2{,}5\ s^{-1} \cdot g^{-1}$
[31]			3·NE 213, γ/n discrimination, BF_3	$<5 \cdot 10^{-2}\ s^{-1}$
[32]			Li glass	$<0{,}01\ s^{-1} \cdot g^{-1}$
[33]			NE 213, $\epsilon \approx 2\%$,	$<0{,}06$–$0{,}10\ s^{-1} \cdot g^{-1}$
			γ/n discrimination	bursts $< 10^3/20$ min
[34]			NE 213, BF_3	Upper limit not indicated $<0.3\ s^{-1}$
[35]	Pd, Ti	Electrolysis, gas phase	NE 213	

TABLE V.

Reference	Metal	Method of saturation	Detectors	Result
[36]	Pd	Electrolysis, D_2 gas 1–20 atm	SNM-14, $\epsilon \approx 3 \cdot 10^{-3}$	$< 2 \cdot 10^{-2}\ s^{-1} \cdot cm^{-3}$ $< 2 \cdot 10^{-3}\ s^{-1} \cdot cm^{-3}$
[27]	Ti	Electrolysis, D_2 gas 50 atm	SNM-14, $\epsilon \approx 3 \cdot 10^{-3}$	$< 10^{-2}$–$3 \cdot 10^{-3}\ s^{-1} \cdot cm^{-3}$ $\Lambda < 10^{-26}\ s^{-1}\ (DD)^{-1}$
[37]	Pd, Ti	Electrolysis	6NE 213, γ/n discrimination $\epsilon \approx 1\%$	$< 5 \cdot 10^{-3}\ s^{-1}$ $\Lambda < 2 \cdot 10^{-25}\ s^{-1}\ (DD)^{-1}$
[38]	Pd		20 ^{3}He, $\epsilon \approx 15$–20%	$< 0.07\ s^{-1} \cdot cm^{-3}$ $\Lambda < 1.5 \cdot 10^{-24}\ s^{-1}\ (DD)^{-1}$
[39]	Pd, Ti		NE213, γ/n discrimination	$< 4 \cdot 10^{-3}\ s^{-1}$
[40]	Pd, Ti		NE 320 + ^{6}Li (15%)	$< 1.5 \cdot 10^{-2}\ s^{-1}$

counting, presented by Fleischmann and Pons. This was shown in Ref. 41 by converting the intensity of the γ-ray line from the calibrated Pu/Be source to the value $\approx 4 \cdot 10^4$ neutrons/s, presented in Ref. 5, and by comparing with the intensity of the γ-ray line claimed by Fleischmann and Pons.

Moreover, from analysis of the γ-ray background for typical laboratory conditions it is concluded in Refs. 41 and 43 that the γ-ray line in Ref. 5 should indeed correspond to 2.5 MeV and not 2.22 MeV.

Additional considerations indicating a possible source of errors in the γ-ray measurements performed by Fleischmann and Pons are presented in Ref. 28. In Ref. 28 a NaI detector was employed and peaks at 2.22 MeV and 2.61 MeV (shown in Fig. 11) were accumulated over a period of 16 h. It is well known that this energy range contains two peaks due to decays of the radioactive elements ^{214}Bi (2.204 MeV) and ^{208}Tl (2.614 MeV). ^{214}Bi is an intermediate product of the radioactive series U–Ra, containing ^{222}Rn. The latter element is present in different types of concrete and in air. The difference between the peaks due to ^{214}Bi (2.204 MeV) and neutron capture (2.224 MeV) cannot be resolved with the help of a NaI counter. For this reason, in their further investigations the authors employed a germanium detector, which is less efficient but has a much higher energy resolution. The spectrum obtained during electrolysis of D_2O is presented in Fig. 12 and shows the presence of a peak due to ^{214}Bi; however, there is no signal at 2.224 MeV. In subsequent experiments, the authors detected, as done in Ref. 41, a peak due to capture of neutrons emitted by a source placed in a paraffin moderator. The result of the measurements is shown in Fig. 13. Two peaks are clearly seen: one at 2.204 MeV, due to ^{214}Bi, and one at 2.224 MeV, due to the reaction p(n, γ)D. In addition, the intensity of the background peak due to ^{214}Bi approximately corresponds to that of the γ-ray peak in Ref. 5. Analogous arguments are also given in Ref. 38. The foregoing considerations show that the γ-ray line indicated in Ref. 5 is apparently a result of instrumental error and is not related with γ-rays from cold fusion.

Other γ-ray data are presented in Table VI.

1.5. Charged particles

The main information on the experiments[19,26,27,38,44,45] on the detection of charged particles is presented in Table VII. We shall make some remarks regarding Refs. 19, 26, and 27. As is well known, protons are quite difficult to detect during electrolysis, because the layer of electrolyte and the cell walls significantly absorb 3-MeV protons. For this reason, the following technique was employed in Ref. 19 in order to investigate the spectrum of scintillations excited by protons. A palladium cathode in the form of a thin strip was removed from the electrolyzer, a fast-neutron detector was unpacked, and the cathode was wound on the lateral surface of an n-terphenyl single crystal and coated on top with a reflecting film. The detector was then placed on a photomultiplier. This problem was solved even more simply in Ref. 26 by the method of ion implantation, in which the space between the source of charged particles (Pd, Ti) and the detectors was a vacuum so that absorption could occur only in the material of the source itself. This made it possible to detect emission not only of protons, but also of T and ^{3}He. Measurements of the emission of charged particles were performed, first, as the target was cooled from the irradiation temperature to $T \approx 77$ K after irradiation stopped and, second, when the target was heated to a high temperature (up to

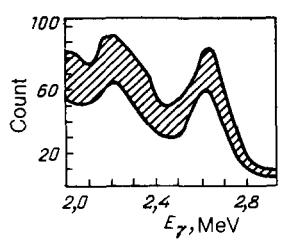

FIG. 11. γ-ray spectrum, measured with a NiI detector.[28]

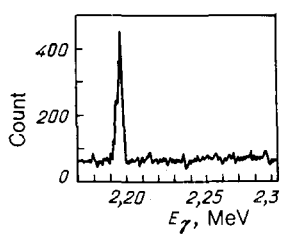

FIG. 12. Same as Fig. 11. Ge detector.[28]

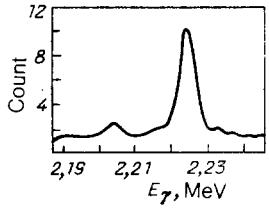

FIG. 13. γ-ray spectrum measured with a Ge detector behind a parafin wall irradiated with a neutron source.[28]

$\approx$750–800 K). After irradiation was stopped, three to five exposures, each with a duration of 10^3 s, were made. During the exposures the deuterium-saturated target was exposed in front of the semiconductor detector and the energy spectrum of the particles emitted by the target was continuously recorded. A quite high value of Λ was found: $5.5\cdot10^{-19}$ and $1.65\cdot10^{-19}$ s^{-1} (DD)$^{-1}$ for Pd and Ti, respectively.

The authors note that the intensity of the emission depends strongly on the experimental conditions. In particular, in the case of exposure directly after irradiation of the target (no heating) the frequency with which signals appear is observed to decrease with time, i.e., the effect disappears. The highest frequency of signals is observed in the period when the target is heated to a high temperature, as a rule, accompanying thermal desorption of deuterium. The last remark concerns Ref. 27. The measurements reported in Ref. 27 were performed in order to check the existence of an exotic "Mössbauer" reaction (see Sec. 3)

$$D+D+Pd\rightarrow{}^4He+Pd' \ (23 \text{ MeV}),$$

in which momentum is transferred to the Pd lattice and energy $\approx$23 MeV is carried off by the α-particle, whose range should be equal to 90 μm in Pd, $\approx$200 μm in Ti, and 350 μm in the material of the CR-39 track detector, employed in Ref. 27.

1.6. X-ray emission

In contrast to most cold-fusion experiments, in which the products of the primary radiation from nuclear fusion (n, p, γ, ...) or capture γ-rays were detected, in Refs. 36, 38, 46, and 47 the x-rays produced when charged particles decelerate in a condensed medium were recorded. This method has the advantage that it is sensitive to all nuclear events, and for this reason in setting up experiments there is no need to make any assumptions about which reactions predominate. In this connection we recall that to explain the discrepancy in the Fleischmann-Pons experiment between the release of heat and the neutron flux different exotic neutron-free reactions (the "Mössbauer" type (see Sec. 3), $D+{}^6Li\rightarrow2\alpha+24$ MeV, etc.) were proposed. If such reactions are the predominant channel of energy release in the crystal lattice, then they are best detected by measuring the x-ray flux. It should be noted, however, that the sensitivity of this method is low. Thus in Ref. 46 it is estimated from the observed values of $\dot{N}_\gamma<0.14$ s^{-1} that $\dot{N}_{nuc}<10^5$ nuclear events per second, which is far from the Jones level.

Information on x-ray-detection experiments is given in Table VIII.

1.7. Analysis for tritium and helium

Many authors have pointed out that the results of Fleischmann and Pons[5] on the detection of tritium are unconvincing, because Fleischmann and Pons give only the final content of T in the electrolyte ($\approx$1.67 Bq/ml) without indicating the initial content of tritium or the duration of electrolysis.

In Ref. 28 several typical samples of heavy water were analyzed. It was found that they contain T in the following quantities (in Bq/ml): 9.5 ± 0.3, 1.1 ± 0.1, 5.8 ± 0.2, and 2.1 ± 0.1. If tritium was present in D_2O at the start of electrolysis, then owing to the effect of D/T separation (which itself is due to the fact that the activation energy of desorption of T on a Pd electrode is different from that of D) the electrode will be enriched with tritium (the enrichment factor $\approx$2–3). The additional formation of tritium owing to background thermal neutrons in the process

$$n+{}^6Li\rightarrow{}^4He+T \ (4{,}78 \text{ MeV})$$

has been found to be negligible compared with the initial content of T in D_2O. The presence of T is detected using its β-decay.

Analysis for the content of helium is performed with the help of mass spectrometry. Thus in Ref. 33 the mass spectrometer made it possible to determine $3\cdot10^4$ and $1.5\cdot10^9$ atoms of ^{3}He and ^{4}He, respectively.

Very interesting positive results with respect to tritium were obtained in Refs. 17 and 25. In a series of experiments,

TABLE VI.

Reference	Measured Energy E MeV	Detector	Result
[13]	2,223	NaI (Tl), $\epsilon=1\%$	Volley $\sim10^2$ s^{-1} "bursts" $2\cdot10^3$ s^{-1}
[20]	2,223	Ge, $\Delta E=2{,}2$ KeV $\epsilon\approx1{,}5\cdot10^{-5}$	<13 s^{-1}
[21]	2,223	NaI (Tl), NE 213 γ/n discrimination	Result for γ not presented (see Table IV)
[30]	2,223	Ge	<50 s^{-1}
[33]	5,5	BGO, $\epsilon=0{,}5\%$	$<0{,}02$ s$^{-1}\cdot$g^{-1}
[36]	5,5	Ge(Li)	$<2\cdot10^{-3}$ s$^{-1}\cdot$cm^{-3}
[38]	5,5 23,8	Ge, NaI(Tl)	$<0{,}05$ s^{-1} (5,5 MeV)

TABLE VII.

Reference	Metal	Method of saturation	Particle, detector	Result
[44]	Pd	Electrolysis	p, Si	$<0{,}074\ s^{-1}\cdot cm^{-3}$
				$\Lambda < 3{,}1\cdot 10^{-24}\ s^{-1}\ (DD)^{-1}$
[45]	Ti	Implantation $E_D = 1{,}5$ KeV	p, surface-barrier	$\Lambda < 8\cdot 10^{-24}\ s^{-1}\ (DD)^{-1}$
[19]	Pd	Electrolysis	p, paraterphenyl	$\gtrsim 10^{2}\ s^{-1}$
[27]	»	»	^{4}He (23 MeV), surface-barrier, track	$\Lambda < 4\cdot 10^{-27}\ s^{-1}\ (DD)^{-1}$
[38]	»	»	p, Ge	Signal not found
[26]	Pd, Ti	Implantation	p, T, ^{3}He, surface-barrier	$\Lambda(Pd) \approx 5{,}5\cdot 10^{-19}\ s^{-1}\ (DD)^{-1}$
				$\Lambda(Ti) \approx 1{,}65\cdot 10^{-19}\ s^{-1}\ (DD)^{-1}$

performed at BARC (Babha Center for Atomic Research, India),[17] the level of T in the electrolytes after several days of continuous operation was measured by two independent groups of experts with the help of the standard technique of liquid scintillators, but taking special measures to prevent spurious effects produced by radioactive contaminants and chemiluminescence. The results obtained by the different groups are presented in Table IX. The conclusion following from these experiments is that the predominant product is tritium, i.e., the cold-fusion reaction can be characterized as being substantially "neutron-free" and having the yield $n/T \sim 10^{-8}$. The radiographic investigations performed by the authors confirm that a significant quantity of tritium is formed and accumulates in the defects of the crystal lattice of the hydride. On the whole, as one can see from Table X, in a number of publications on the search for T and He it is concluded that cold fusion does indeed exist.

1.8. Calorimetric measurements

As we have already pointed out above, the sensational interest in the work of Fleischmann and Pons stems primarily from their calorimetric results, which showed significant excess energy production during electrolysis of D_2O. Reports confirming these data soon appeared in many laboratories.[49,50]

Most of these investigations have never been published. Instead, there appeared numerous publications in which, based on detailed measurements and careful analysis it is concluded that there is no positive heat effect at a level many orders of magnitude lower than that indicated by Fleischmann and Pons.[5] Possible sources of error in Ref. 5 have been indicated and it has been demonstrated that the effects found by Fleischmann and Pons can be explained by well-known chemical processes, which have nothing in common with nuclear fusion.

We emphasize that the phenomena occurring in the cell comprise a complicated series of different electrochemical processes and calorimetry requires that many factors be taken into account accurately: polarization effects, shift of the electrode potential, loss of heat owing to formation and escape of gases, evaporation of D_2O, different types of nonsteady-state phenomena, etc.

Figure 14 (taken from Ref. 51) shows two types of calorimetric cells that can be employed to measure the production of excess heat.

In the cell shown in Fig. 14a, in which the cathode and anode spaces are separated, the diaphragm does not prevent the transfer of ions, but it does prevent the movement of gas bubbles between the anode and the cathode. When the gas space above the cell is completely separated and the gas flows are separately directed out of the cell, recombination in the gas phase is impossible. The transfer of dissolved gases is not very significant because the solubility of the gases is low ($< 10^{-3}$ moles/liter). To eliminate different nonsteady-state effects electrolyte must be periodically added and its level must be maintained constant.

In the closed cell (Fig. 14b) the amount and composition of the electrolyte are constant. The gases formed transform back into water as a result of catalytic recombination. Under these conditions energy storage in the products of electrolysis does not occur and the energy supplied is completely transformed into heat. When additional sources of energy production are present, the total released power should exceed the supplied electric power. To eliminate errors associated with the differences in the conditions under which the measurements are performed the thermal equiva-

TABLE VIII.

Reference	Metal	Method of saturation	Detector	Result
[46]	Pd	Electrolysis	Si (Li)	$<10^{6}\ s^{-1}\cdot cm^{-3}$
[47]	Pd	»	NaI (Tl), Ge	Small excess above background
[36]	Pd	»	Ge	Effect not observed
[38]	Pd	»	NaI (Tl), Ge	$< 10^{2}$ events$\cdot s^{-1}\cdot cm^{-3}$

TABLE IX.

Metal	Volume of D_2O, ml	Maximum current A	Level of T, Bq/ml		Formation	
			Initial	Final	Bq	atoms
Pd—Ag	250	100	2,6	$5,6\cdot10^4$	$1,4\cdot10^7$	$8\cdot10^{15}$
Pd—Ag	250	100	10,0	$4,4\cdot10^3$	$1,1\cdot10^6$	$6\cdot10^{14}$
Pd	1000	65	2,0	$7,0\cdot10^3$	$7,0\cdot10^6$	$4\cdot10^{15}$
Ti	135	40	2,0	$1,8\cdot10^3$	$2,4\cdot10^5$	$1,3\cdot10^{14}$
Pd	45	1—2	31,3	$1,7\cdot10^4$	$7,5\cdot10^5$	$4\cdot10^{14}$
Pd	65	1—3	18,1	$8,8\cdot10^3$	$5,7\cdot10^5$	$3\cdot10^{14}$

lent of the supplied electric power can be determined in a completely identical experiment but using ordinary water, in which case excess heat should not be produced. It should be kept in mind, however, that the substitution $D_2O \rightleftarrows H_2O$ gives a correct check only if the differences in the properties of the electrolytes based on D_2O and H_2O are taken into account (the difference in the heat capacities, the thermal conductivities, the masses of the gases released, and the electrical conductivity and the resistance of Pd with respect to H_2O and D_2O). This makes the interpretation of difference measurements in the systems Pd/H and Pd/D very difficult and delicate.

The calorimetric cell employed by Fleischmann and Pons is of a type that falls between the types shown in Figs. 14a and b. Because of this there arise difficulties and ambiguities in the interpretation of their measurements. The first detailed analysis of these results was performed by Kreysa, Marx, and Plieth.[28] Kreysa *et al.* repeated the measurements many times and they did not observe excess heat within the limits of accuracy of the measurements ($\pm 5\%$) in any of their attempts. In all cases a palladium cathode was completely submerged in the electrolyte. When the electrode saturated with deuterium or hydrogen was removed from the electrolyte it was found that its surface heated up. This is a consequence of the release of D(H) from the electrode and oxidation of D(H) in the presence of a catalyst. In their energy calculations Fleischmann and Pons neglected the contribution of this reaction to catalytic recombination (CR)

$$2D_2 + O_2 \rightarrow 2D_2O, \quad H_{CR} = -147{,}3 \text{ kJ/mole of } D_2.$$

In Ref. 28 the recombination heat was measured. For a $0.1\times1\times2$ cm^3 Pd electrode the heat flux was equal to 35.9 W, and the flux density of catalytic recombination was equal to 179.6 W·cm^{-3}. This is significantly higher than the "excess" flux density ≈ 10 W·cm^{-3} presented in Ref. 5. The authors call attention to the fact that catalytic recombination of the hydrogen stored in Pd does not always occur and its appearance and rate depend on the catalytic activity of the surface of Pd.

In addition to catalytic recombination, heat can also be released owing to the absorption of H(D) itself by the palladium:

$$nD_2 + Pd \rightarrow Pd \ldots D_{2n}, \quad H' = -18{,}4 \text{ kJ/mole of } D_2.$$

If the equilibrium content of H(D) is achieved in the electrodes, then this effect can be neglected, since the release of heat owing to absorption of D_2 is compensated by the heat absorbed on desorption. Under non-steady-state conditions, however, this effect must be taken into account.

Fleischmann and Pons employed a combined cell, containing a mixture of hydrogen and oxygen in the gas phase above the electrolyte. It can be conjectured[28] that part of the surface of the palladium electrode rose above the level of the electrolyte and thus came into contact with oxygen throughout the entire experiment or during a time when the electrolyte level decreased owing to the electrolytic decomposition of water. Catalytic recombination could have appeared on the exposed parts of the electrode. Because catalytic recombination depends strongly on the catalytic activity of the Pd surface different non-steady-state phenomena can occur. Such phenomena can be observed as "bursts of heat." The tendency of the "excess" heat release to increase as the current density j increases, as found in Ref. 5, can also be easily explained, since the release of heat accompanying catalytic recombination $Q_{CR} \sim j$. Finally, catalytic recombination can explain the "volume" character of the heat effects indicated in Ref. 5, since the amount of H(D) entering into the catalytic recombination reaction will increase as V/S increases.

Other possible sources of errors in calorimetric mea-

TABLE X.

Reference	What is recorded, method	Result
[28]	T, liquid scintillator	Effect not found
[48]	T, ^{3}He, mass spectrometer	T, ^{3}He found
[33]	T, ^{3}He, ^{4}He, liquid scintillator, mass spectrometer	$<3\cdot10^2$ ^{3}He s$^{-1}\cdot$g^{-1} $<4\cdot10^5$ ^{4}He s$^{-1}\cdot$g^{-1}
[17]	T, liquid scintillator, radiography	$\dot{N}_T > 10^{16}/10^3$ s
[18]	T, ^{3}He, mass spectrometer	$\dot{N}_T > 10^2$ s^{-1}
[19]	T, ^{3}He, mass spectrometer	10^2 s^{-1}
[25]	T	10^{13} s$^{-1}\cdot$cm^{-3}
[35]	^{3}He, ^{4}He	Effect not found
[38]	T, ^{3}He, ^{4}He, liquid scintillator, mass spectrometer	$(5\pm7)\cdot10^1$ T s$^{-1}\cdot$cm^{-3}, above-background ^{3}He, ^{4}He signal not found

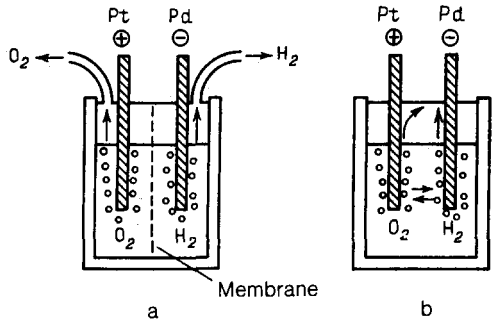

FIG. 14. Two types of calorimetric cells.

surements have also been identified.[38,52]

a) A sharp or gradual change in the rate of heat loss from the cell can arise as a result of a change in the rate of gas formation. Such effects often result in an increase of the temperature of the cell; this can be interpreted as excess enthalpy.

b) When the electrolyte is not well mixed, temperature gradients can appear, and if these temperature gradients are neglected, errors can arise in the calculations of the heat balance.

c) The total electrical energy supplied to the cell can vary in the course of an experiment as a result of changes in the temperature and concentration, random screening of the electrodes by gas bubbles, etc. It is difficult to estimate this energy accurately in the course of a long experiment.

d) In order to determine the amount of electrical energy that is dissipated into heat it is necessary to know the "instantaneous" value of the resistance of the electrolyte, and it is by no means trivial to determine this value.

Different types of calorimeters are employed in calorimetric experiments on cold fusion. These calorimeters are predominantly used to perform measurements in the equilibrium state. The sensitivity of the best calorimeters is $\pm$ 100 μW.[33] On the whole, the typical accuracy of calorimetric measurements, as a rule, falls in the range 5–7%.

Figure 15 shows, as an example, a diagram of the calorimetric apparatus employed at the Paul Scherrer Institute (Switzerland)[33] to perform equilibrium measurements of the heat generated in a cell. Heat is removed with the help of gas flowing through the cooling jacket on each cell. The heat generated is measured based on the difference arising in the temperatures of the gas as the gas flows through the jacket. This design makes effective mixing unnecessary. The only deviation from equilibrium in the experiment was connected with the gradual reduction of the volume of the electrolyte. This reduction was compensated by periodically adding D_2O into the main cell and H_2O into the control cell.

Of all the published calorimetric experiments with which I am familiar (Refs. 23, 25, 28, 33, 35, 38, 49, 51, 53, 54) an indication of excess heat at a level of 5–15% was obtained only in Refs. 23, 25, 35, and 49. Based on the remarks made above there are no grounds for regarding the results as confirming the heat effect.[5]

1.9. Experiments on the mechanical fracture of deuterium-containing materials

In this section we shall examine Refs. 9 and 55–57, in which the possibility of the appearance of nuclear fusion reactions accompanying mechanical fracture of materials containing deuterium was studied. The first investigation, Ref. 9, was carried out three years before Fleischmann and Pons performed their work and at the time it did not attract any appreciable attention. In the light of the ideas on the acceleration mechanism of cold fusion[7,8] (if they are ultimately confirmed experimentally) this work can now apparently be regarded as the first experimental work on cold (more accurately, microscopically hot) nuclear fusion.

The purpose of the work was to check the assumption that nuclear reactions can be initiated by shock-induced fracture of LiD single crystals. This material was chosen because the structure of lithium deuteride is similar to that of alkali-halide crystals, which become strongly electrified when they fracture.

A diagram of the experimental apparatus is shown in Fig. 16. The LiD crystals were fractured with a metal pile drive with a mass of 50 g *(1)*, which was accelerated in the barrel of a gas gun *(2)* to a velocity of about 200 m/s. The target consisted of a 7 mm thick lead plate *(3)*, on one side of which a conical pit, 5 mm deep, was made. A LiD single crystal *(4)* in the form of a cube with 3 to 4 mm long edges was placed into this pit. The crystal was covered with a thin brass cover *(5)*.The target was secured to the vertical wall of the chamber *(10)*.

Neutrons were detected with the help of a block of seven NWI-62 proportional counters *(6)*, submerged in a tank containing oil *(7)*; the walls of the tank were covered with a sheet

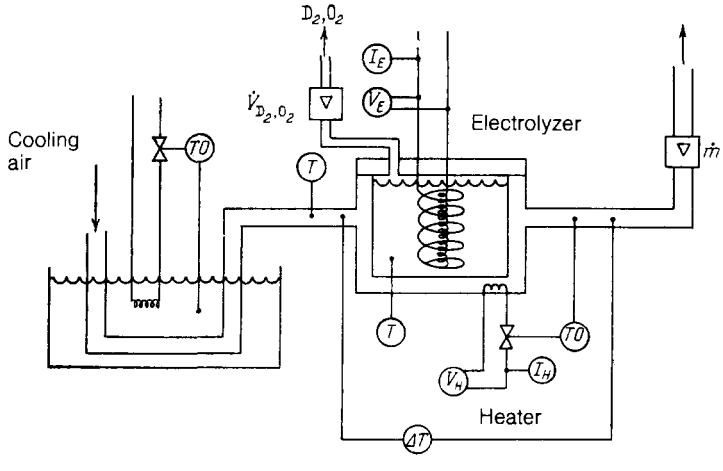

FIG. 15. Calorimetric apparatus of Ref. 33.

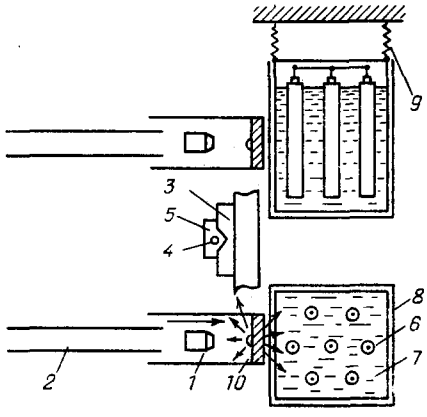

FIG. 16. Diagram of experimental apparatus.[9]

of cadmium *(8)*; and, the tank itself was suspended with the help of a spring suspension *(9)*. The detector efficiency was estimated with the help of a Po/Be neutron source with an intensity of 200 neutrons/s; the neutron source was positioned at the location of the target. The natural neutron background was recorded in regular time intervals. For control, the background with shots on the targets not containing LiD crystals (the so-called pulsed background) was also measured.

The measurements are summarized in Fig. 17. They show that the neutron count in the case when the target contained LiD is higher than the pulsed background count and is of the order of 10 neutrons per act of fracture of the LiD single crystal.

Experiments on "rheological explosion" of rocks to which D_2O was added were performed at approximately the same time by M. A. Yaroslavskiĭ at the Institute of Terrestrial Physics of the Academy of Sciences of the USSR. These experiments gave a similar result: observation of intense neutron emission accompanying fracture of deuterium-containing samples. The results of these investigations were published only in 1989.[55]

Due to reports of the observation of cold fusion in the

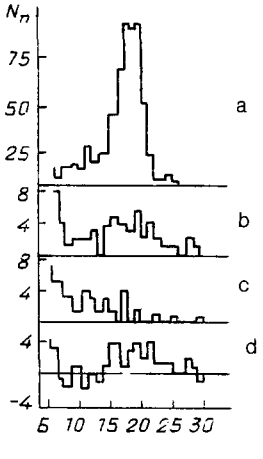

FIG. 17. Histogram of the distribution of pulses over the channels of the analyzer: neutron source (a), with fracture of lithium deuteride targets (b), with shots on targets not containing LiD crystals, "pulsed" background (c), and the result of subtracting the "pulsed" and cosmic-ray backgrounds from the amplitude spectrum measured with fracture of LiD targets (d).

case when Pd and Ti are saturated with deuterium, Deryagin's group returned to their investigations and in 1989 they reported the detection of a neutron flux[56] and anomalous β activity[57] accompanying mechanical action on titanium in the presence of deuterium-containing substances. In both experiments titanium shavings, D_2O, and deuterated polypropylene PP (D_6) were studied, while in Ref. 6 lithium deuteride (LiD) was also studied. These materials were ground down and mixed in a laboratory eccentric vibrating mill. As a control, all components were also ground down separately; this showed that when only the titanium shavings themselves as well as the deuterium-containing components were dispersed separately, no excess above the natural background (≈ 0.05 counts/s) is observed. (Note that this result, as applied to LiD, does not agree with preceding measurements performed by the same group,[9] who observed neutron emission accompanying fracture of LiD.) At the same time, when the titanium shavings are dispersed together with 10% heavy water or 4–5% deuterated polypropylene (D_6) as well as when both components are dispersed together the intensity of the neutron count, taking into account the efficiency of the detector, is five to six times higher than the intensity of the cosmic-ray background. The largest effect is observed in the system Ti + 10% D_2O + 4% PP (D_6), when the working drum is frozen in liquid nitrogen 3 to 6 min after the mechanical action stops, and is equal to 0.40 ± 0.14 counts/s. After three or four 3-min cycles of vibrational dispersing the neutron count drops to the natural neutron background, and it is not restored by subsequent mechanical action.

As the authors point out, saturation of Ti with deuterium in this experiment can occur owing to mechanochemical decomposition of deuterium-containing components and diffusion of deuterium into the Ti lattice in the presence of significant contact pressures. The increase in the neutron count on freezing could be connected with the fact that the equilibrium phase pressure of H(D) drops as the temperature decreases; this results in an increase of the absorption of deuterium. The observed reduction of "neutron generation" is apparently caused by both strong fragmentation of Ti and poisoning of its surface, which prevents diffusion of deuterium into the Ti lattice.

When the formation of tritium was investigated, vibrational dispersing of copper with the same deuterium-containing substances, taken in the same proportion to the weight of the metal, was performed together with a control procedure under analogous conditions. It was found that in the system Ti + 10% D_2O + 4% PP (D_6) an excess of 40 to 50% above the natural background and the backgrounds of the control samples Cu + 10% D_2O and Cu + 4% PP (D_6) is observed.

In concluding this section I would like to point out that in contrast to most work on cold fusion the experiments on "mechanical fracture" were actually performed only by one group and require further and more extensive checking.

1.10. Summary of experimental investigations

The following conclusions can be drawn based on the experimental data studied in this section.

1. The results of calorimetric measurements [excess heat release at a level of ~ 1 W·cm^{-3} (Ref. 5)] performed by Fleischmann and Pons have not been confirmed. No heat

effect was observed at the level of accuracy of the order of 1%. From the standpoint of possible nuclear reactions, this imposes quite weak limits on their rate ($\lesssim 10^{10}$–10^{11} $s^{-1}\cdot cm^{-3}$). For practical applications, however, this result is critical, because it leaves no hope for the application of cold fusion for commercial power production.

2. Negative results were also obtained on the detection of 23.8 MeV and 5.5 MeV γ-rays as well as x-rays. What do these results mean? As will be shown in Sec. 3 of this review, the rate of the reaction (4B), leading to γ (23.8 MeV), is five orders of magnitude lower than that of the reactions (2B) and (3B). The rate of the reaction (1B), which gives γ (5.5 MeV), depends on the conditions of fusion. For cold fusion (the characteristic energies of the fusing nuclei ~ 1 eV) it must be ~ 2 orders of magnitude higher than for the reactions (2B) and (3B), while for hot fusion (energies of 1–10 keV) it must be four to five orders of magnitude lower. As regards the x-rays, as pointed out above, the detection of x-rays is not as sensitive as direct detection of neutrons. Thus the absence of the indicated signals does not contradict the existence of cold fusion, but the result for γ (5.5 MeV) supports the hot-fusion model.[2)]

3. The results obtained for all other detection channels (see Fig. 5) confirm the existence of cold fusion. The average intensity of the process, in most cases, was close to the Jones level, though in some cases it can be several orders of magnitude higher during short time intervals.

4. An interesting feature, possibly the key feature for understanding the nature of cold fusion, are the "neutron bursts"—emission of a large number of neutrons (tens and hundreds) within short time intervals (fractions of a second); these bursts are observed together with temporally uncorrelated neutron emission.

5. A characteristic feature of successful cold-fusion experiments is that the process is sporadic: the samples become "active" soon after the onset of saturation or thermal cycling (tens of minutes to several hours) and the activity decreases with time. This fact could cast light on the reason for the lack of success in some experiments in which the activity was measured tens and hundreds of hours after onset of saturation.

6. Another important observation is that the intensity of the cold fusion process depends on the conditions of the experiment (the rate of sorption and desorption, the range and rate of change of the temperatures, the state of the surface, etc.). There is no doubt that nonequilibrium conditions in the metal-deuterium system are critical for the appearance of cold fusion.

7. A remarkable characteristic of the experiments performed at BARC[17] (and the University of Texas[25]) is the finding that cold fusion is predominantly of a neutron-free character and results in the formation of tritium in the ratio $T/n \sim 10^8$.

The results following from the experimental observations examined above in order to understand the mechanism of cold fusion will be discussed in detail below.

In spite of the enormous number of investigations which, on the whole, confirm the existence of cold fusion, the experimental investigations of this phenomenon are still at a stage when the experimenters cannot reliably reproduce their results and create conditions guaranteeing the observation of cold-fusion signals. A number of observations need to be checked in detail. Thus the conclusion that tritium is predominantly generated in cold-fusion reactions deserves very careful study. Obviously, this is now the most urgent problem. It is also very important to obtain confirmation of the, as yet, few results on the detection of the charged products of cold fusion. Unfortunately, there are still no data on correlation experiments,[3)] proposed in Refs. 7 and 8, on simultaneous detection of the products of cold fusion and the associated signals (radio and acoustic emission). The effect of different external factors on the course of cold fusion has also not been studied much.[7,8] In some experiments thermal cycling, which is apparently important for obtaining positive results, is employed. There are also indications that cold fusion is activated by "electric shock" (strong pulsating current). In general, extensive experimental investigations must still be performed before cold fusion has been adequately studied and understood.

2. HYDRIDES OF TRANSITION METALS

For the purposes of the subsequent discussion, we shall study in this section (following Ref. 8) some questions concerning the structure, formation, and decomposition of metal hydrides. We shall focus our attention on transition metals, which can dissolve large amounts of hydrogen and its isotopes. We shall study primarily palladium and titanium, in which, according to the publications examined in Sec. 1, cold-fusion reactions are observed. A more complete exposition is given in numerous monographs, reviews, and original papers devoted to metal-hydrogen systems (see, for example, Refs. 58–62).

2.1. The structure and bonds in metal-hydrogen systems

Hydrogen forms different types of bonds with metals. Hydrides of the most active alkali and alkaline-earth metals have the structure of halides and are characterized by an ionic bond. In the case of rare-earth metals hydrogen forms compounds with covalent and metallic bonds, while in the case of transition metals hydrogen forms predominately bonds of the metallic type. These latter compounds are often regarded as interstitial solutions, in which hydrogen atoms, which are relatively small, occupy voids between the metal atoms in the lattice. In the process, the properties of both the metal and hydrogen change significantly, i.e., chemical interaction occurs.

The filling of interstitial positions in the metal lattice by hydrogen atoms results in deformation of the lattice and the formation of a displacement field. Hydrogen in a metal can be in different phase states: gas, liquid, and solid. The first two states differ only by the hydrogen density and the lattice constant of the metallic matrix. The solid phase is characterized by ordering of the hydrogen interstitials over equivalent interstices.

In cubic lattices hydrogen can occupy two types of interstices—octahedral, in which the hydrogen atom is surrounded by six metal atoms, and tetrahedral, in which a hydrogen atom is surrounded by four metal atoms. In addition, for every metal atom there are one octahedral and two tetrahedral voids, whose size for an undistorted fcc lattice is related with the atomic radius of the metal by the expression

$$R_0 \approx 2R_T \approx 0.44R_m. \qquad (2.1)$$

The ionic radius of hydrogen depends on the type of bond in which hydrogen participates: $R_H^{(c)} \approx 0.30$–0.35 Å for a covalent bond, $R_H^{(i)} \approx 1.3$–1.5 Å for an ionic bond, and $R_H^{(m)} \approx 0.41$ Å for a metallic bond. The radius of electronegative hydrogen decreases continuously as the electronegativity of the cation increases, and for transition hydrides it is equal to ≈ 1.23 Å for Pd, ≈ 1.25 Å for Ti, and ≈ 1.33 Å for La. On the average, for transition metals $R_H^{(m)} \approx 1.29 \pm 0.5$ Å.[58] The effective charge on the hydrogen atom can assume different values ranging from $+1$ to -1, depending on the position of the partner element in the periodic system. Accordingly, the electronic properties of the metal-hydrogen systems are often described with the help of two alternative models: anionic, in which hydrogen attracts to itself an electron from the metal and is transformed into a negative ion H^-, and protonic, in which hydrogen gives up its electron to the conduction band and transforms into a positively charged proton. In real systems an intermediate situation can be realized [thus, in palladium hydrogen apparently has, on the average, a charge of $+0.45e$ (Ref. 63)]. This means that in transition metals hydrogen is not found in the form of a bare proton, but rather each hydrogen atom has from 0.1 to 0.6 electrons per atom. The remaining electrons, not bound in hydrogen, participate in a residual metallic bond, which determines the electric conductivity of these compounds.

We shall now study titanium and palladium in greater detail. The hydrides of these metals are among the best studied hydrides. The capability of palladium to absorb large quantities of hydrogen has now been known for more than 150 years. The systematic study of the diffusion of gases in metals started with Graham's investigations of Pd in 1866.[64] As regards the hydrides of Ti, their detailed study has led to wide applications of this metal in technology and has opened up the possibility of storing hydrogen in the hydride phase.

Palladium hydride has the structure of an isotropically expanded fcc lattice of the metal. Below 300 °C the uniform solid solution decomposes into the α phase with a low content of hydrogen ($c_\alpha^{\max} = 0.008$) and β phase with a high concentration of H ($c_\beta^{\min} = 0.607$) and a larger lattice constant. At room temperature the values of the lattice constant for pure Pd and coexisting α and β phases are $a_{Pd} = 3.890$ Å, $a(c_\alpha^{\max}) = 3.894$ Å, $a(c_\beta^{\min}) = 4.025$ Å. The transition $\alpha \rightarrow \beta$ is accompanied by an increase in the volume of the hydride $\Delta V = 1.57\ \text{cm}^3/\text{g}\cdot\text{atom}\cdot\text{H}$.[62] As the hydrogen concentration increases above $c_\beta^{\min}$ the homogeneous phase expands smoothly. Since the atomic radius of Pd is equal to $R_{Pd} = 1.34$ Å, we find from Eq. (2.1) for the sizes of the octahedral and tetrahedral voids

$$R_0^{(Pd)} \approx 0.6\ \text{Å}, \quad R_T^{(Pd)} \approx 0.3\ \text{Å}.$$

One can see that for $R_H^{(m)} = 0.41$ Å hydrogen can be easily distributed in the octahedral voids of the Pd matrix and does not "climb into" the tetrahedral voids. The formation of the α- and β-hydride phases occurs precisely owing to the filling of octahedral positions whose complete filling corresponds to the limit $c \rightarrow 1$.

Thus far we have neglected the differences between hydrogen and its isotopes—deuterium and tritium. It should be noted that palladium hydrides containing D and T exhibit the inverse isotopic effect, i.e., the equilibrium pressure of D and T in them is higher than that of H at the same temperature and with the same composition. Thus it is more advantageous for deuterium, than hydrogen, to be in a gas while it is more advantageous for hydrogen to be in a metal.[62] However, for the further discussion these differences are not significant and, unless otherwise stated, we shall not distinguish below between H, D, and T in metals.

The compound TiH_2 is the most interesting, from the standpoint of cold fusion, hydride phase of titanium with the highest concentration. The γ phase, which exists at temperatures $T < 310$ K, has an fct lattice with $a = 4.528$ Å and $c = 4.279$ Å while the γ' phase ($T > 310$ K) has an fcc lattice with $a = 4.454$ Å in the case of $TiH_{1.99}$ and $a = 4.440$ Å in the case $TiD_{1.99}$.[58] We note that the atomic radius of titanium $R_{Ti} = 1.46$ Å, so that the sizes of the voids in the fcc lattice are $R_0 \approx 0.64$ Å, $R_T \approx 0.32$ Å $< R_H^{(m)} = 0.41$ Å. Nevertheless, structural investigations show that in both ordered γ and γ' phases of titanium hydride hydrogen fills tetrahedral voids. Thus the possibility of hydrogen absorption in titanium (and its analogs) is limited to two hydrogen atoms per metal atom, in spite of the fact that, generally speaking, three interstitial positions are accessible. (We note that an analogous situation also occurs for group-V metals: V, Nb, and Ta.) We shall return to this question below.

2.2. Transfer of hydrogen in a metal and formation of a hydride layer

In the investigation of metal-hydrogen systems saturation with hydrogen (or its isotopes) is conducted by different methods: from a gaseous medium under pressure, electrolysis, ion implantation, and gas or spark discharge. In many experiments on cold fusion the first two methods have been most popular; these methods are quite simple and make it possible to achieve high deuterium concentrations. We shall briefly discuss the basic characteristics of diffusion of hydrogen in metals. It is well known that the penetration of hydrogen into a metal is preceded by adsorption of hydrogen molecules on the surface of the metal and a transition into the chemisorbed state, close to an atomic state but with some nonzero effective charge on the hydrogen atoms. Diffusion of hydrogen atoms into the crystal lattice starts after the hydrogen has interacted with the surface layer of the metal and the metal dissociates. Hydrogen is highly mobile in the metal, and its diffusion coefficient in transition metals is close to that in liquids. In describing diffusion it can be assumed that the matrix atoms are stationary and form a crystalline basis in which the hydrogen "lattice gas" spreads. Diffusion can be regarded as a process in which hydrogen atoms hop from one interstitial position to another, overcoming in the process the energy barrier produced by the compression of the interstitial atom by the surrounding metal atoms. Neglecting quantum effects, it can be assumed that the diffusion is caused by the thermal vibrations of the interstitial atom and the height of the barrier ε depends on the elastic energy of the matrix and the size of the interstitial atom. The diffusion coefficient satisfies Arrhenius' law

$$D = D_0 e^{-\varepsilon/RT}. \tag{2.2}$$

For the α-hydride of Pd $D_0 \approx 6 \cdot 10^{-3}\ \text{cm}^2\cdot\text{s}^{-1}$ and $\varepsilon \approx 25$ kJ·mole^{-1}, for the α phase of the hydride of Ti $D_0 \approx 10^{-2}$ cm^2·sec^{-1} and $\varepsilon \approx 52$ kJ·mole^{-1}, while for the phase

TiH_{2-x} the value of D_0 is approximately an order of magnitude lower.[65]

In the presence of a concentration gradient and external forces F, acting on the interstitial atoms, the total hydrogen flux through the sample can be represented in the form

$$j = j_{\text{dif}} + j_{\text{drift}} = -nD \operatorname{grad} C + nCMF; \tag{2.3}$$

here n is the number of atoms of the lattice per unit volume and M is the mobility of the interstitial atoms. The electric current, produced by an electric field $E = \operatorname{grad} \Phi$, results in the appearance of a force F, whose value can be expressed in terms of the phenomenological effective charge Z^* of the interstitial atom: $F = -eZ^*E$. The fact that two force components act on the interstitial atom is taken into account in this relation. One component is determined directly by the force field and includes static screening and polarization effects. The second component (the "electron wind") appears as a result of the interaction of the interstitial atom with the conduction electrons drifting in the external field.

Similarly, when a temperature gradient is present there arises a force $F = -(Q^* \operatorname{grad} T)T^{-1}$, where Q^* is the heat of transfer. The time dependence of the local concentration $C(r, t)$ is described by the equation

$$\frac{\partial C}{\partial t} = D\Delta C - MF \operatorname{grad} C, \tag{2.4}$$

where it is assumed that D, M, and F do not depend on r. The main features of hydrogen transfer in cold-fusion experiments can be easily understood by studying a very simple and quite typical example of diffusion with $F = 0$ in a flat plate ($l_y, l_z \gg l_x$). In this case the diffusion flux depends only on x and is determined by the concentration gradient. Assuming that the hydrogen concentration at $x = 0$ and $t \geqslant 0$ is constant and equal to C_0 and that the diffusion coefficient D does not depend on C, we obtain the well-known solution of the problem with a constant source:

$$C(x, t) = C_0 e^{-x^2/4Dt}. \tag{2.5}$$

The time over which diffusion stops is equal to

$$\tau_{\text{dif}} = \frac{L^2}{D}, \tag{2.6}$$

where L is the characteristic distance over which C varies. Note that when the drift term $MF \cdot \operatorname{grad} C$ predominates the time required to complete the transfer process is determined by the relation

$$\tau_{\text{drift}} \approx \frac{L}{MF}. \tag{2.7}$$

The process is diffusive, if

$$LF < kT.$$

In our case the situation is complicated by the fact that when the metal is saturated with hydrogen (deuterium) different hydride phases, whose diffusion coefficients D_{hi} are, generally speaking, different from the diffusion coefficient D_m of the metal, form. The dynamics of these processes is studied in Ref. 67. The solution can be easily found, if it is assumed that hydride forms around a point x immediately after a certain hydrogen concentration $C = C_h$ is reached. We shall assume that the concentration C_0 is constant in the entry surface layer and that the diffusion coefficients D_m and D_h are independent of C.

From Eq. (2.5) we find the time dependence of the penetration depth of the hydride:

$$x_{\text{h}}(t) = 2\left(D_{\text{h}} t \ln \frac{C_0}{C_{\text{h}}}\right)^{1/2} \tag{2.8}$$

and the concentration at the exit surface of the metallic plate

$$C_{\text{exit}}(t) = C_{\text{h}} \exp[-(l - x_{\text{h}}(t))^2 (4D_{\text{m}})^{-1}], \tag{2.9}$$

where l is the thickness of the plate.

If several hydride phases with different values of the diffusion coefficients can coexist, the solutions of the type (2.8) and (2.9) must be joined at the boundaries of the phases. Expansion of the lattice in the transverse plane (y, z) and especially along the x axis can change the character of the diffusion somewhat. For us, however, in what follows it is more important that an increase in the dimensions of the lattice in the hydride layer results in the appearance of stresses, which for some critical thickness of the hydride layer lead to cracking of the material. Because the cracks formed are filled with hydrogen, the hydrogen flow along the x axis drops sharply, after which it is gradually restored as the cracks are filled. After a new layer of hydride grows up to the critical thickness, a new cycle of cracking occurs. Such "wavelike" phenomena have been observed experimentally, for example, in the case of diffusion of hydrogen in titanium in a gas-discharge plasma.[67]

2.3. Fracture accompanying absorption of hydrogen

We shall now study some questions connected with the fracture of metals accompanying absorption of hydrogen. In any method of hydrogen absorption the energy of the hydrogen atoms is of the order of several electron volts, which is sufficient to overcome the surface potential barrier. Further penetration of hydrogen into the material under the action of diffusion and external fields is accompanied by deformation of the lattice and, in some cases, fracture of the material. We stress that the possibility of fracture in the absence of an external mechanical load is not obvious; it is determined by the chemical interaction of hydrogen with the material, the properties of the crystalline phases arising, the rate of diffusion, the kinetics of the formation of microcracks, etc. In this respect our problem is substantially different from the problem of fracture of materials under irradiation, when energetic external particles directly create defects in the lattice as a result of the development of a cascade, the formation of strongly ionizing recoil nuclei, "heat peaks," etc.[68,69]

As a result of diffusion and the formation of hydride phases the distribution of hydrogen atoms as well as stresses and strains that are established in the material are highly nonuniform. Since the lattice constants of the hydride phase are different, stresses arise not only within the phases but also at the boundaries between them. Further, after the onset of fracture hydrogen is intensively packed into the cracks, and this generates an additional rupturing stress. In polycrystalline samples, in addition, the intense diffusion of hydrogen along grain boundaries and in dislocations and other defects is very significant. On the whole, there arises a very complicated dynamic picture of the interacting processes of diffusion and formation of hydrides and cracks. This picture is also complicated by the fact that hydrogen changes the

properties of the materials (this is especially important in the region of the tip of a crack). For sufficiently plastic materials, hydrogen increases the hardness and embrittlement.[70]

The general conditions for hydrogen-induced fracture of a brittle material are formulated in Ref. 71.

First, hydrogen absorption should occur up to concentrations sufficient to produce significant "swelling" of the entire lattice. These concentrations are usually close to those at which a hydride forms.

Second, the local stresses generated by hydrogen absorption must be close to the fracture stresses.

Third, the material must be saturated with hydrogen under conditions when the relaxation of the local stresses can be neglected (i.e., at sufficiently low temperatures).

The characteristic relative strains accompanying saturation with hydrogen $\varepsilon = (a_2 - a_1)/a_2$, where a_1 and a_2 are lattice parameters in different phases. Then, according to the kinetic theory of fracture, the fracture time (longevity) of the material is given by

$$\tau_{\text{frac}} = \tau_0 \exp\left[C_a (\varepsilon^* - \varkappa\varepsilon)(\alpha kT)^{-1}\right], \tag{2.10}$$

where C_a is the atomic heat capacity, α is the linear expansion coefficient, T is the temperature, ε^* is the maximum fracture strain, and $\varkappa$ is the local-overload factor, which takes into account the fact that the local stresses in the material can be significantly higher than the average stresses. Here it is conjectured that from the standpoint of fracture (its starting stage—at the level when microcracks form) the internal expansion stresses play the same role as external stresses. Unfortunately the longevity estimated from the formula (2.10) is very uncertain, since the parameter τ_0 is extremely small and the exponential is large. For example, for parameters characteristic for intermetallides of the type FeTi ($\tau_0 = 10^{-13}$ s, $C = 3k$, $\alpha = 10^{-5}$ K^{-1}, $\varepsilon^* = 0.2$, $\varepsilon = 0.083$, $T = 300$ K) we obtain[71]

$$\tau_{\text{frac}} \sim 10^{-13} C \cdot \exp\left[200\left(1 - \frac{\varkappa}{2{,}4}\right)\right]. \tag{2.11}$$

The uncertainty in the parameter $\varkappa$ ($1 \leqslant \varkappa \leqslant 2.4$) results in a very large uncertainty in τ ($\tau \sim 10^{38}$–10^{13} s). It is thus necessary to appeal to experiment, making the assumption that the fracture time is determined by diffusion of hydrogen and the formation of hydride, which fractures virtually immediately. Then, according to Eq. (2.6) with $L = 10^{-2}$ cm and $D = 10^{-8}$ cm$^2 \cdot$s^{-1} (at room temperature) we obtain the characteristic fracture time $\tau \sim 10^4$ s. As regards the cracks that are formed, their size, according to diverse experimental data, is approximately 10^4–10^5 Å. This is indicated, in particular, by the fact that under prolonged hydrogen absorption ($\sim$1 h) some materials (of the intermetallides type) decompose into a powder with these characteristic particle sizes.

There are many theoretical and experimental studies on the fracture of materials accompanying hydrogen absorption. Most of them are concerned with the technical problems of storing hydrogen in metals or fatigue fracture of materials under a load in a hydrogen atmosphere. However a complete quantitative theory of this process still does not exist. For purposes of further discussion it is sufficient to make the following assumptions, which are in agreement with the experimental data:

1) The characteristic fracture depths L and fracture times τ of a material are related by the diffusion relation $L^2 \sim D\tau$. This means that the lifetime of the hydride phase is neglected compared with the diffusion time.

2) As a result of fracture cracks with the characteristic sizes $l \sim 10^4$–10^5 Å and $d \sim 10^3$–10^4 Å in the longitudinal and transverse directions, respectively, form.

3) We shall assume that the number of cracks n_c per unit volume is sufficient to give the observed swelling of the material accompanying hydrogen absorption $\Delta V/V \sim 0.1$. If the average volume of a crack is v_0, then $n_c \sim \Delta V/Vv_0$. A microcrack is usually assumed to be close to a flat disk, and then $v_0 \sim l^2 d \sim 0.1 l^3 \sim 10^{-13}$–$10^{-10}$ cm^{-3}, $n_c \sim 10^{12}$–10^9 cm^{-3}.

We stress the fact that the cracks under study should not be given too literal a meaning. In reality the fracturing of a material is a much more complicated process, and the quantities l, d, v_0, and n_c describe only its average characteristics. For example, the total area of the surfaces formed on cracking (per unit volume) is of the order of $\sim l^2 n_c$, while the width of cracks having a complicated shape is $\sim d$.

3. THEORETICAL ASPECTS OF COLD FUSION

The most important question in the theoretical interpretation of experiments on cold fusion is: What is the mechanism by which under the conditions of "low-temperature experiments" the Coulomb repulsion is overcome with adequate efficiency so that nuclei can approach one another to distances $R_{\text{nuc}} \sim 10^{-13}$–$10^{-12}$ cm at which nuclear forces giving rise to fusion operate? Based on the foregoing discussion of cold-fusion experiments, "adequate efficiency" means that the rate of fusion reactions at the Jones level is achieved, i.e., $\Lambda \sim 10^{-24}$–10^{-23} fusions per second per DD pair; this corresponds to a neutron yield in the channel (2B) $\sim 10^{-2}$–10^{-1} neutrons per second per gram of cathode matter.

3.1. Coulomb barrier. Fusion in nuclear collisions

Curve 1 in Fig. 18 depicts schematically the internuclear Coulomb repulsion potential

$$U_{\text{Conl}} = \frac{Z_1 Z_2 e^2}{R} \tag{3.1}$$

between two nuclei, having charges $Z_1 e$ and $Z_2 e$ of the same sign and separated by a distance R. If the energy of the relative motion of the nuclei is equal to E and $Z_1 = Z_2 = 1$, then the minimum "classical" separation R_0 of the nuclei is equal

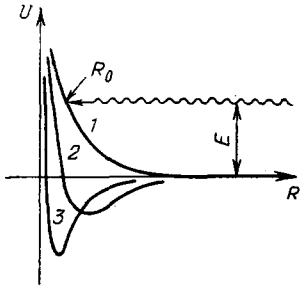

FIG. 18. Schematic diagram of the Coulomb repulsion potential of two deuterium nuclei without screening (1), with electronic screening (2), and with muonic screening (3).

TABLE XI.

Reaction	S_0, MeV·b	A, $cm^3 \cdot T^{-1}$	A, $s^{-1} \cdot molec$	A/A (DD)
$D+D \to {}^3He+n$, $T+p$	0,11	$1,5 \cdot 10^{-16}$	$3 \cdot 10^{-64}$	1
$p+D \to {}^3He+\gamma$	$2,5 \cdot 10^{-7}$	$5,2 \cdot 10^{-22}$	10^{-55}	10^{-5} (10^2)
$D+T \to {}^4He+n$	11,5	$1,3 \cdot 10^{-14}$	10^{-69}	10^2 (10^{-2})

to

$$R_0 \approx \frac{14\text{Å}}{E(\text{eV})}. \tag{3.2}$$

At energies of the order of 1 eV, corresponding to chemical reactions, R_0 is equal to several angstroms. Nuclear forces, which lead to fusion, operate at significantly shorter distances $R_{nuc} \sim 5$–10 fm $= (5\text{–}10) \cdot 10^{-13}$ cm. Quantum mechanics makes it possible for nuclei to approach one another to such distances by means of tunneling. The fusion cross section σ is determined by the product of the nuclear cross section σ_{nuc} and the tunneling probability P:

$$\sigma = \sigma_{nuc} P. \tag{3.3}$$

For low energies ($\lesssim 10^2$ keV) σ_{nuc} can be parameterized in the form

$$\sigma_{nuc} = \frac{S(E)}{E}, \tag{3.4}$$

where $S(E)$ is a slowly varying function: $S(E) \approx \text{const} = S_0$. The values of S_0 for the reactions (1B), (2B), (3B), and (5B) are presented in Table XI.[72] The Gamow factor P at low energies can be written in the form

$$P = e^{-\alpha}, \quad \alpha = 2\int_{R_n}^{R_0} k(r)\,dr, \tag{3.5}$$

where $k(r) = [2\mu(V(r) - E)]^{1/2}$ is the local wave number. Substituting (3.2) we find

$$\alpha = 2\pi e^2 \left(\frac{2E\hbar^2}{\mu}\right)^{-1/2} = \pi \left(\frac{2\mu}{m_e}\frac{R_0}{a_0}\right)^{1/2} \approx 44{,}4\,[E\,(\text{keV})]^{-1/2}; \tag{3.6}$$

here μ is the reduced mass, $a_0 = \hbar^2/m_e e^2 \approx 0.51$ Å is the Bohr radius, and the last expression was written for the (DD) reaction.

The energy dependence of the cross sections of the reactions (1B), (2B), (3B), and (4B) in the energy range $E \approx 10$–10^3 keV, corresponding to "hot" conditions ($T \approx 10^8$–10^{10} K), is shown in Fig. 19.[73] One can see that in this region the cross section of the reaction (5B) has the highest value; this is caused by the existence of the ^{5}He resonance. The cross section of the process (1B) has the lowest value; this is connected with the smallness of σ_{nuc}, determined by the emission of γ-rays.

As E decreases the Coulomb barrier becomes increasingly more important. The tunneling probability is determined primarily by the width of the barrier (i.e., $R_0 - R_{nuc}$), which increases as E decreases, which causes the exponent α in Eq. (3.5) to increase. As a result P is very sensitive to the value of the reduced mass μ: reactions with small values of μ become preferable. Correspondingly, the ratio of the reaction probabilities changes. Thus for "bare" nuclei (i.e., no screening by electrons)[74]

$$\sigma(DT) < \sigma(DD) \quad \text{for } E < 40 \text{ eV},$$
$$\sigma(pD) > \sigma(DD) \quad \text{for } E < 200 \text{ eV}.$$

This means that the relative rates of different reactions will be completely different for cold and hot fusion.[75] We shall return to this question somewhat later, after we discuss the effects of screening.

With the help of the relations (3.3) and (3.6) it is possible to estimate the energy of a collision of bare deuterium nuclei that could result in fusion at the Jones level. The experimental conditions can be modeled by assuming that a flux of deuterons with energy E and strength 1 A strikes a target containing deuterons with density $\rho = 4 \cdot 10^{22}$ cm^{-5}. Then

$$\frac{dN}{dt} = \frac{I}{I_0}\rho v \sigma, \tag{3.7}$$

and the result of Jones *et al.*[6] corresponds to $E \approx 0.35$–0.4 keV.[76] Thus the energies that are required to explain cold-fusion experiments based on the standard "collisional" mechanism (neglecting screening) are of the order of $E \sim$ keV.

It should be kept in mind that the estimates of Ref. 76 are very arbitrary, because in these estimates the fact that the target contains, apart from deuterium, metal atoms, which make up the crystal lattice, is neglected. The presence of these atoms imposes a significant restriction on the efficiency of fusion in crystalline targets. The energy of the incident deuterons is expended primarily on electromagnetic interactions (excitation and ionization of atoms), whose cross section σ_{el} is significantly larger than the nuclear cross section σ_{nuc}: $\sigma_{nuc}/\sigma_{el} \sim 10^{-8}$. Since in each collision the energy of the incident deuteron decreases by $\Delta E \sim E_{ion,exc} \sim 1$–$10$

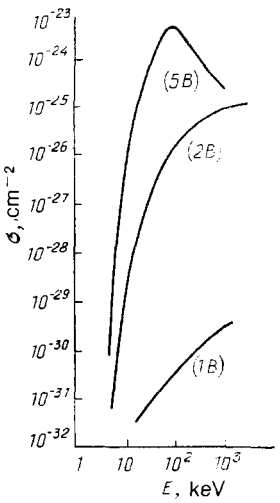

FIG. 19. The energy dependence of the cross sections of the reactions DD (2B), DT (5B), and pD (1B).

eV, the range of deuterons with energy $E_d \sim 1$–10 keV is $\delta \sim (E_D/\Delta E)a_0 \sim (3\text{–}4)\cdot 10^3$ Å.

The question of the possibility of energetically favorable nuclear fusion under conditions when crystalline targets are irradiated with a beam of accelerated particles was investigated by Kuz'min and Vysotskiĭ[77,78] long before the experiments of Fleischmann and Pons. Kuz'min and Vysotskiĭ noted that the quantum and thermal fluctuations of the atoms in the crystalline matrix result in deformation of the matrix and can lower the Coulomb barrier and thereby increase the probability of tunneling through the barrier. The same idea was later stated in Ref. 79.

3.2. Bound-state fusion

The probability of fusion can be increased if the separation of the nuclei is decreased or the width of the barrier is lowered in some manner.

3.2.1. Fusion in a D_2 molecule. We shall first study the D_2 molecule. The electronic bond results in modification of the Coulomb barrier and the appearance of a bound state, as shown schematically by curve 2 in Fig. 18. The minimum of $V(r)$ corresponds to an equilibrium distance $R_{D_2} \approx 0.74$ Å between the deuterium nuclei. The "equivalent" energy, which could lead to such a separation of the nuclei without electronic screening is $E^{eqv} \approx 20$ eV. The rate of fusion is determined by the probability that the nuclei approach one another to a distance R_{nuc}:

$$\Lambda = A\,|\,\Psi(R_{nuc})\,|^2; \tag{3.8}$$

here Ψ is the normalized wave function, describing the relative motion of the nuclei, and the constant A is expressed in terms of S_0:

$$A = \frac{S_0}{\mu c^2}\frac{c}{\pi\alpha}, \quad \alpha = \frac{e^2}{\hbar c}. \tag{3.9}$$

The wave function $\Psi = \psi/4\pi r$ can be found by solving the Schrödinger equation

$$\left(-\frac{\hbar^2}{2\mu}\frac{d^2}{dr^2} + V(r)\right)\psi(r) = E\psi(r), \quad \int_0^\infty \psi^2(r)\,dr = 1. \tag{3.10}$$

The electronic screening at short distances makes it necessary to replace Eq. (3.1) by

$$V(r) = \frac{e^2}{r} - V_0. \tag{3.11}$$

The electronic energy of the D_2 molecule is very close to that of an isolated ^{4}He atom [$E(^4\text{He}) = -79.0$ eV]. The quantity V_0 is therefore determined by the difference of $E(^4\text{He})$ and the binding energy (27.2 eV) of two D atoms, i.e., $V_0 = -51.8$ eV. At large distances the potential for a diatomic molecule can be employed.[80,81] Solving Eq. (3.10) numerically gives[72] the values of A and Λ in the third and fourth columns of Table XI. I call attention to two facts. First, the values of Λ(DD) found in Refs. 72 and 82 are approximately ten orders of magnitude larger than the values obtained in earlier calculations,[83,84] where the "shift" of the potential V_0 at short distances was neglected. Second, owing to the smaller reduced mass Λ(pD) is eight orders of magnitude larger than Λ(DD).

3.2.2. "Compression." As one can see, the probability that the D nuclei in a D_2 molecule fuse is negligibly small for $R_{D_2} \approx 0.74$ Å. One attempt to understand cold fusion is based on the assumption that in a crystal the nuclei approach closer to one another. How close should they approach in order for cold fusion to be significantly accelerated? This was estimated first in Ref. 83 and recently in Refs. 75 and 76. For example, two nuclei and an electron can be placed into a sphere of radius R, outside which the wave functions are required to vanish;[76] as R decreases the internuclear separation decreases, the energy of the ground state increases, and the amplitude of the wave function at the origin increases. For a rough estimate, however, the expression (3.6), which takes into account explicitly the dependence of P on the width of the barrier R_0, is adequate. Then it is easy to prove that Λ can be increased from $3\cdot 10^{-64}$ s^{-1}, corresponding to a D_2 molecule with $R_{D_2} = 0.74$ Å, up to $\sim 10^{-24}$–10^{-23} s^{-1} (the Jones level) by decreasing R_{D_2} by approximately a factor of five. The value $R_x \approx 0.3a_0 \approx 0.125$ Å (Refs. 75 and 76) gives the order of magnitude of the internuclear separation required to explain cold fusion.

3.2.3 Ratio of the rates of different reactions in cold and hot fusion. It is interesting to compare the relative rates of different reactions in the hot and cold fusion regimes. As the typical hot conditions we shall study the collision of bare nuclei with the relative energy $E \sim 10$ keV ($T \sim 10^8$ K). At this energy, as one can see from Eq. (3.2), the width of the Coulomb barrier is $R_0 \approx 144$ fm. For cold fusion we shall assume that some specific screening conditions allow deuterium nuclei, placed in a crystal, to approach one another to the distance $R_0 \approx R_x \approx 0.125$ Å $\gg R_0$ ($E = 10$ keV). In this case the rate of fusion is determined by the expression[75]

$$N_x = \nu S_0 \frac{k(R_{nuc})}{k(R_e)} \exp[-\alpha(R_{nucl}, R_x)]; \tag{3.12}$$

here ν is the vibrational frequency, which determines the collision frequency; R_e is the equilibrium distance; $k(R_e)$ is the wave number of zero-point vibrations; and, $\hbar^2 k^2(R_e)/2m_e \approx h\nu$. The relative rates of the reactions pD and DT with respect to the reaction DD, which were calculated in Ref. 75, are presented in the last column of Table XI. The first numbers correspond to hot fusion and the second numbers (in parentheses) correspond to cold fusion.

3.3. Screening in metals

We shall now discuss the question of whether electrostatic screening in crystals can increase the rate of nuclear fusion. This question has been analyzed in a number of studies.[82,85–89] The general conclusion to which the authors of these papers arrive is that there are no grounds for assuming that the crystal lattice of Pd, Ti, ... contains positions at which there exist strong electric fields, capable of holding deuterium nuclei at distances significantly shorter than in a normal diatomic molecule D_2. We recall that the shortest distance between neighboring deuterium atoms at octahedral interstices in PdD is equal to ≈ 2.9 Å. For this reason it is obvious that the question of the required internuclear separation is relevant only if a pair of deuterons is placed at one and the same interstitial position. The electrostatic field, necessary for holding pairs of positive charges at a distance of, for example, 0.6 Å (i.e., somewhat shorter than $R_{D_2} \approx 0.74$ Å), is equal to 0.78 a.u. At the same time, as the calculations of Refs. 86 and 87 show, for example, for an

octahedral cluster P_D^{2-}, the electrostatic potential at a local minimum, corresponding to the center of an octahedral void, is 0.17 a.u. while at a distance of 0.5 Å away from the center it is equal to 0.14 a.u.

Moreover, as shown in Ref. 88, placing a D_2 molecule into a Pd cluster results not in compression of the cluster, but rather expansion by approximately ≈ 0.2 Å.

It is interesting to estimate the electronic density ρ_x that could create the required screening. The value of ρ_x can be found[88] with the help of a simple model of screening in a metal, in which the electron sea is described in the Thomas-Fermi approximation. In the linear approximation, for a uniform electron density ρ the bare Coulomb potential (3.1) is screened to the value

$$\frac{e^2}{r} e^{-k_0 r}, \tag{3.13}$$

where

$$k_0^2 = 4\left(\frac{3}{\pi}\right)^{1/3} \rho^{1/3} a_0^{-1}.$$

As we saw above, the required rate of fusion can be obtained by decreasing the characteristic size of the D_2 molecule by a factor of ≈ 5, or (see Sec. 3.4) $m_e \to m^* \approx 5m_e$, i.e., $a_0 \to a_0^* \approx a_0/5$. It is obvious that the same effect can be obtained by increasing ρ, but this time by a factor of $(5)^3$ compared with the molecular density $\rho_{mol} \sim 2e[(4/3)\pi(0.74)^3]^{-1} \approx 1.2e$ (Å)$^{-3}$, i.e., $\rho_x \approx 125\,\rho_{mol} \approx 150e$ (Å)$^{-3}$. This value is completely unrealistic, because, for example, the electron density in an octahedral void in Pd is[90] $\rho_{oct} \approx 0.8e$ (Å)$^{-3}$.

High electron densities can exist only within Pd atoms, but D^+ nuclei should be strongly repelled from these regions by the repulsive core of Pd, whose charge is equal to $+46e$.

We recall, finally, the very stringent and quite general restrictions, derived in Ref. 89, on the possible intensification of the screening of the DD Coulomb barrier in metals in the equilibrium state. The authors showed that if the effective repulsion of two D atoms at short distances were indeed significantly weakened by some solid-state effects, then the same effects should significantly intensify the binding of ^{4}He with metals, which is not observed experimentally. Thus, though screening in metals undoubtedly affects the probability of fusion of the nuclei, it cannot completely explain the experimentally observed rate of cold fusion. In attempting to find a way out of this difficult situation Rafelski *et al.*[76] and Garel *et al.*[91] suggest that some dynamic effects, owing to the combined effect of screening and the motion of the deuterium nuclei within the metallic lattice in the process of sorption or desorption, could be at play.

3.4. Screening and catalysis by heavy particles

It is obvious that electronic screening becomes more effective if the electron distribution is localized in a smaller region around the positively charged nucleus. This, however, should at the same time increase the kinetic energy. This fact limits the effectiveness of screening, since $E_{kin} \sim (mr^2)^{-1}$ and the (negative) potential energy is $\sim (r)^{-1}$. The kinetic energy could be reduced, if the mass of the electron could be increased. In other words, a negatively charged particle with mass $m^* > m_e$ can form with the nucleus an atom whose Bohr radius is $\sim m^*/m_e$ times smaller than that of a standard atom. This cuts off the Coulomb potential at short distances $R^* < R_e$ and thus increases the probability of tunneling. Figure 20 shows the results of a calculation of the rate of fusion in a (DDe^*) molecule as a function of the mass m^*.[76,82] One can see that even if m^* increases moderately, Λ increases very rapidly. In particular, Λ at the Jones level can be obtained with $m^*/m_e \approx 4$–5;[72,76,82] this, by the way, is also obvious from Eq. (3.6). Based on similar considerations, attempts were made in Refs. 92–94 to approach the problem of screening in a metal, making the assumption that it is caused by "heavy electrons"—quasiparticles, which are introduced in the theory of metals. If such particles are localized between some pairs of deuterium nuclei, then this could result in the screening of the DD repulsion. However, as was pointed out, for example, in Ref. 74, the concept of a "heavy electron" is connected with nonlocal electron-lattice interactions. At distances $R \sim R_{nuc} \ll 1$ Å these quasiparticles cannot give the required screening, because they have a spatially extended structure and at short distances their effective mass reduces to the bare electron mass.

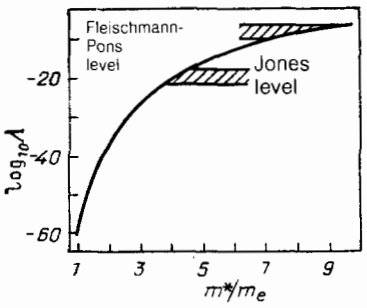

FIG. 20. The rate of fusion as a function of the mass m^*.[76,82]

Another possibility is connected with the proposition made in Ref. 95 that cold-fusion reactions are initiated by cosmic muons (we recall that $m_\mu \approx 207m_e$), which "get stuck" in the hydride and catalyze fusion. The idea of muonic catalysis has a long history. F. C. Frank noted back in 1947 that Coulomb repulsion can be screened by a negatively charged muon captured in an atomic orbital. Soon after this, Sakharov and Zel'dovich[97–99] proposed using this phenomenon for muonic catalysis of nuclear fusion, since a muon, hopping from one nucleus to another during its lifetime ($\tau_\mu \sim 2.2 \cdot 10^{-6}$ s^{-1}), can play the role of a catalyzer. (We note that $R_{DD\mu} \approx 4 \cdot 10^{-3}$ Å and $\Lambda_{DD\mu} \approx 10^{11}$ s^{-1}). Muonic catalysis is now one of the promising paths for solving the problem of generating electricity based on nuclear fusion.[100]

More detailed estimates[74] show, however, that catalysis by cosmic muons can hardly explain the experiments on cold fusion. Since the flux of stopped muons (≈ 0.1 g$^{-1}\cdot$h^{-1}) is small, the relative fraction of muons captured by the deuterons is small, and the muon lifetime τ_μ is short, and taking into account the losses owing to "attachment" to helium, it turns out that one muon can catalyze only a small number (~ 20) of DD fusions. Even for the most favorable conditions this results in $\dot{N}_{nuc} < 10^{-3}$ s$^{-1}\cdot$g^{-1}. This is significantly lower than the Jones level $\sim 10^{-1}$ s$^{-1}\cdot$g^{-1}. As far as we know, experiments performed in the mountains also do

not confirm this hypothesis.[4)] Of course, if fusion were to be catalyzed by some stable particles, then the limitations associated with the lifetime would not arise.

The existence of stable heavy charged particles is indeed predicted in some theoretical models, though as yet there is no experimental evidence for them. The possibility of using in practice such hypothetical particles, which could be produced in accelerators and then used for catalyzing nuclear fusion, has been discussed in a number of articles.[101-103] However it was shown in Ref. 104 that existing models of acceleration, even under the most favorable conditions, do not permit solving this problem. Catalysis of cold fusion with the help of stable heavy particles requires either the development of new methods for producing such particles or using them in "ready form," if they exist and can be accumulated under natural conditions. This last possibility is discussed in Ref. 105. It is conjectured that there exist free stable antiquarks $Q \equiv \bar{u}\bar{u}$ (they have an electric charge of 4/3 and a mass of several GeV and they interact with hadrons via a short-range strong repulsive interaction), which, similarly to muons, could catalyze DD fusion:

$$(QDD)\text{-molecule} \rightarrow {}^4He + Q + 23.9\,MeV, \quad (3.14a)$$
$$\rightarrow {}^3He + n + Q + 3.3\,MeV, \quad (3.14b)$$
$$\rightarrow T + p + Q + 4.0\,MeV. \quad (3.14c)$$

In contrast to muons, $Z_Q = -4/3$ ($Z_\mu = -1$) and M_Q is of the order of several GeV ($m_\mu \approx 100$ MeV). As a consequence of this difference, DDQ molecules should form and fusion processes should proceed significantly more rapidly than in muonic catalysis. The charge of the system (DQ) is equal to $-1/3$ [while the system (Dμ) is neutral]. For this reason the molecule D + (Dμ) can form as a result of Coulomb attraction. If the rate of fusion is not limited by the density of D, the fusion cycle time is very short $\approx 10^{-10}$ s. Another feature of the model—the fact that the channel (3.14a) is $\sim 10^4$–10^5 times stronger than the channels (3.14b) and (3.14c)—follows from phase-space considerations, the massiveness of the particles, and the postulated character of the interaction of the particles with the nuclei. This enabled the authors to explain the predominantly neutron-free character of cold fusion. The released energy ~ 1 W corresponds to $\sim 10^{12}$ reactions (3.14a) (or 10^7–10^8 neutrons per second) and requires $\sim 10^2$ "active" Q. The concentration $n_Q/n_{Pd} \sim 10^{-28}$, necessary to explain experiments on cold fusion at the Jones level (and even at the Fleischmann-Pons level), is consistent with the experimental data on free quarks. However, this model is obviously quite exotic, and the existence of the particles Q with the required properties does not follow from any currently existing experimental data.

3.5. Nuclear effects

Another direction in the search for the mechanism of cold fusion involves attempts to explain it by some characteristic features of the nuclear interaction at extremely low energies. Thus a number of authors[94,106,107] have called attention to a possible connection between cold fusion and the "looseness" of the deuteron, whose size, $R_D \approx 4 \cdot 10^{-12}$ cm, is much greater than the range of nuclear forces in the triplet state $R_{tr} \approx 1.7 \cdot 10^{-13}$ cm.[94] As a result, fusion reactions at low energies could proceed primarily by means of the penetration of a neutron into the nucleus, for which process there is no Coulomb repulsion (the Oppenheimer-Phillips effect[108]), thereby making the neutron-free channel (3B) the dominant channel. Simple estimates show, however, that this effect is hardly capable of substantially increasing the rate of fusion, since the characteristic "separation" of n and p in D $R_D \sim 10^{-12}$ cm $\ll R_0^{CF} \sim 10^{-8}$ cm and the binding energy of the deuteron (≈ 2.2 MeV) is significantly higher than the energy characteristic for cold fusion.

In another hypothesis cold fusion is connected with a possible increase in the rate of fusion as a result of a hypothetical narrow nuclear resonance (^{4}He)* near the threshold of the decay of ^{4}He into two deuterons (23.8 MeV).[107,109] The significant enhancement of the cross sections for some fusion reactions as a result of the existence of narrow resonances at low energies is well known; in particular, it plays an important role in astrophysical nucleosynthesis. If the width of the hypothetical resonance (^{4}He)* is very small (10^1–10^2 eV), then the relative variation of the fusion cross section as a function of the energy near threshold can be large. If, however, such a resonance has the typical nuclear width $\Gamma \sim 0$ (MeV), then the lifetime of the DD system in the resonance state $(\Gamma)^{-1}$ is significantly shorter than the time required for tunneling through the Coulomb barrier and the resonance effect is insignificant.[107]

3.6. "Mössbauer fusion"

In studying the different nuclear reactions that could occur during electrolysis (see Table I), Christos[110] came to the conclusion that none of these reactions can explain the energy release unaccompanied by the emission of neutrons or γ-rays. Consider, for example, the reactions (3B) and (6B), which do not give neutrons and γ-rays. The range of protons with $E_p \approx 3$ MeV is equal to ≈ 0.005 cm in Pd and ≈ 0.02 cm in water. The range of 1 MeV tritium is an order of magnitude shorter. For this reason, these particles could at the same time bring about, without leaving the cell, the release of heat in the cell. However the Coulomb excitation of Pd nuclei by 3-MeV protons should result in the emission of $\sim 10^4$ γ-rays with energy ~ 0.5 MeV per second per 1 W via the channel (3B).[111] In addition, the channel (2B), whose probability should be comparable, would also give $\sim 10^{12}$ neutrons per 1 W. Energetic tritons from (3B) should lead to generation of fast neutrons with $E_n \approx 14$ MeV in the channel (5B) ($\sim 10^8$ neutrons per second per 1 W). Finally, the reaction (6B) should lead to the formation of energetic neutrons accompanying the interaction of α particles with $E_\alpha = 11$ MeV with Pd nuclei ($\sim 2 \cdot 10^4$ neutrons per second per watt).

To resolve this inconsistency, Walling and Simons[92] and Hagelstein[112] proposed the so-called "Mössbauer" reaction

$$D + D + (Me) \rightarrow {}^4He + (Me)' + 23.8\ MeV; \quad (3.15)$$

here (Me) designates the "metallic environment," in which the fusion reaction occurs and which absorbs the momentum transferred in the reaction (3.15). In the process the α particle carries off the released energy ≈ 23 MeV. Since the range of α particles in a metal is very short ($\approx 90\,\mu$m in Pd and 200 μm in Ti), the entire energy of the α particle is transformed into heat. The suppression of the channels (2B) and (3B) in

this model is explained as follows. When two deuterons fuse an intermediate ^{4}He nucleus forms first. Under ordinary conditions this nucleus decays into ^{3}He + n or T + p, which ensures that energy and momentum are conserved. In the electrode the momentum is transferred to the lattice. Since ^{4}He is stable, there is no reason for it to decay into ^{3}He + n or T + p. It is obvious, however, that in order for the cross section of the reaction (3.15) to be higher than the cross sections of the reactions (2B) and (3B) the ^{4}He-lattice bond must be unexplainably strong. In addition, the model does not explain the mechanism by which fusion is initiated. In attempting to solve both problems at the same time Walling and Simons[92] proposed that "heavy electrons" play the key role in cold fusion. These electrons, accumulating around deuterons, not only screen the Coulomb repulsion, but they also carry off the energy released in the reaction (3.15). We already spoke about the inconsistency of the model with "heavy electrons" for screening. Unfortunately, it also cannot explain "nonradiative relaxation." Indeed, for energies of ~ 20 MeV electrons in a solid give up virtually all of their kinetic energy to high-energy bremsstrahlung, a large part of which should escape from the cell and be detected by detectors. As the estimates of Ref. 111 show, in the process (3.15) there should arise $\sim 10^6$ γ-rays with an energy of ~ 0.5 MeV per joule of energy from the interaction of ^{4}He with Pd atoms. Thus the enormous difference between the energy released in the reaction (3.15) (of the order of MeV) and the characteristic excitation energy of the lattice (of the order of eV) makes the proposition of "Mössbauer fusion" in the channel (3.15) completely implausible.

3.7. Possible sources of spurious effects

We have already mentioned some studies in which attempts were made to explain the results of cold-fusion experiments in terms of effects that are unrelated to cold fusion (catalytic recombination, isotopic separation of T/D, and catalysis by cosmic muons). We shall now discuss some suggestions of this kind. Although these phenomena cannot explain entirely all experimentally observed features of cold fusion, they must be kept in mind when analyzing the possible spurious effects and backgrounds.

a) In Ref. 113 J. M. Carpenter calls attention to the possible contribution of neutrons produced by cosmic-ray particles (primarily protons) in the atmosphere or in the material surrounding the detectors. The main contribution comes from the evaporation of neutrons from nuclei undergoing collisions with cosmic-ray particles and having energies $E_n \approx 1$–3 MeV. In addition, there are thermal neutrons, which are produced as a result of moderation in the surrounding space to energies $E_n \approx 0.1$ eV, as well as "epithermal" neutrons, having the spectrum $N_n \sim E^{-1}$ at energies in the range $E_n \sim 1$ eV–1 MeV. The flux of each such component is of the order of 10^{-2} neutrons$\cdot$cm$^{-2}\cdot$s^{-1} at sea level and varies with altitude [$\sim \exp(-h/1.5\ \text{km})$] and time, primarily owing to the change in the density of the atmosphere, solar activity, and the geomagnetic field ($\sim \exp[-P/(150\ \text{g/cm}^2)]$); for example, $\Delta P = \pm 13$ mm Hg gives ΔI_n of $\pm 10\%$. In such a flux the shielding and the materials of the detector can be sources of neutrons, whose flux is comparable in magnitude to the signal in cold-fusion experiments. In addition, it should be kept in mind that the energy of the peak due to evaporated neutrons is close to that of the neutrons in the reaction (2B).

b) Another source of spurious neutron signals in cold-fusion experiments could be dissociation reactions of deuterons caused by α particles arising in the decays of radioisotopes in the U, Th, and radon chains.[114] Alpha particles from ^{212}Po (8.8 MeV, Th chain, $\tau(^{212}\text{Po}) = 0.3\,\mu$s) and ^{214}Po (7.8 MeV, U chain, $\tau(^{214}\text{Po}) = 150\,\mu$s) can make the largest contribution. These α particles give rise to the reaction (the threshold is equal to 6.6 MeV)

$$\alpha + \text{D} \rightarrow \alpha + \text{n} + \text{p}. \tag{3.16}$$

Radon, which is present in air, is also a danger. The materials used in buildings contain radionuclides and continuously emit radon. Similarly to other gases, radon is easily adsorbed in different materials and leads to the formation of ^{214}Po or ^{212}Po ($\tau_{\text{Rn}} \approx 3.82$ days).

The variations observed in the neutron counting rate in cold-fusion experiments could be caused by intermittent release of Rn together with gases from the cell. Analogously, when Ti is saturated with deuterium from the gas phase the cold titanium adsorbs Rn several orders of magnitude better. The reactions (3.16) can proceed intensively in the presence of compressed deuterium. The subsequent vanishing of the neutron signal could be due to the decay of Rn. In electrolysis using LiOH the lithium also can give fast neutrons owing to the reaction (α, n).

c) The surrounding γ-rays could also cause photodisintegration of deuterons or other nuclei, resulting in neutron emission. In this respect (like also for the sources studied above) simple removal of the cell is not an adequate method for monitoring the neutron background, just like the substitution of H_2O for D_2O.[115]

I stress once again the fact that the signal observed in most cold-fusion experiments is weak, as a rule at the level of the background. For this reason, the experiment must be performed carefully in order to eliminate spurious sources of fast and slow neutrons and γ-rays, careful decontamination must be performed, materials with low levels of radioactive impurities must be used, and the background conditions of the experiment must be studied in detail.

3.8. Conclusions

The analysis performed in this section shows that for steady-state systems there is no mechanism based on the standard ideas of nuclear and solid-state physics that can explain the results of experiments on cold fusion, even at the Jones level. In the next section we shall study a possible version of a substantially nonequilibrium "acceleration" mechanism that, being quite simple and natural, is capable of explaining the basic features of cold fusion.

4. ACCELERATION MECHANISM OF NUCLEAR FUSION

4.1. The acceleration mechanism and the properties of hydrides

In this section we shall examine scenarios of the "acceleration mechanism" of cold fusion in transition-metal hydrides. This model, which was proposed in Ref. 7, has been analyzed in detail in Ref. 8. Here we shall follow the presentation given in Ref. 8. The idea that the phenomenon of cold fusion is based on an acceleration mechanism has also been

posited in a number of other papers [Refs. 74,107,116–120].[5)] In Refs. 9, 56, and 57 it was posited in connection with mechanical fracture of crystals.

The acceleration mechanism of cold fusion[7] has been posited based on two experimental observations: a) the appearance of microcracks when hydrogen is absorbed in metals (Pd, Ti, ...) that strongly absorb hydrogen and its isotopes and b) mechanoemission, accompanied by the fracture of different crystalline materials and adhesion layers. The first of these phenomena has already been discussed in Sec. 2. It is well known from work with hydrides, and it is caused by the increase in the dimensions of the starting metallic lattice when hydrogen (or its isotopes) is dissolved in it, by the appearance of mechanical stresses, and by the loss of plasticity of the hydride phase.

The mechanoemission of electromagnetic waves, accompanied by fracture of crystals and adhesion layers, has also been investigated in many experiments (see, for example, Ref. 11). These phenomena are usually interpreted based on the idea that charges, which generate an electrostatic field, appear on the edges of the cracks. It is conjectured that the electrostatic field generated in this manner is capable of accelerating electrons and ions present in the gap up to energies of ~ 1–10^2 keV and can also give rise to field emission of electrons, which is what produces the experimentally observed bremsstrahlung and characteristic emission.

Thus one would think that when metals are saturated with deuterium up to high deuterium concentrations conditions that are favorable for the occurrence of cold-fusion reactions can be created. In reality, numerous microcavities form in deuterium-rich hydride, and these microcavities are also filled with deuterium ions. If it is assumed that as cracks open up strong electric fields are generated, as happens when ionic crystals fracture, then these fields can accelerate the deuterium ions and impart to them the energy necessary to overcome the Coulomb barrier. However, a number of questions arise in any attempt to transfer the acceleration mechanism in this manner directly to transition-metal hydrides. As we have already mentioned in Sec. 2, the properties of stable hydrides of the type PdH, TiH_2, etc., which have been studied, point to the fact that they form bonds of the metallic type. In this case the answer to the basic question of how the surfaces of the cracks are charged becomes unclear. In ionic crystals charges appear when ionic bonds break as cracks form along crystalline planes, as a result of which the opposite edges of cracks acquire charges having different signs. The picture is not so obvious for crystals with a metallic bond. In addition, the "microcapacitor" that is formed in this manner should rapidly discharge through the surrounding hydride mass, since at room temperature the resistivity of the hydrides PdH, TiH_2, ... is virtually identical to that of the corresponding metal (numerical estimates will be given below in Sec. 4.2). Finally, field emission from the metal should occur in the presence of the strong fields (up to $E \sim 10^8$ V/cm) that can arise in cracks, and it should result in discharging of the "microcapacitor." Over this period of time a heavy particle (deuteron) can acquire only a small energy $W_D \sim (m_e/m_D) W_D \sim (1$–$10^2)$ eV, which is not high enough to overcome the Coulomb barrier with the required efficiency.

We shall study below, following Ref. 8, some physical phenomena which nonetheless can also give rise to the acceleration mechanism for the case of the transition-metal hydrides of interest to us.

In Ref. 8 it is posited that in the course of the nonequilibrium process in which transition metals are saturated with hydrogen (D, T) there arises an unstable hydride phase, in which the metal is transformed into an insulator (or semiconductor). In reality, such phenomena, in which dielectric properties are enhanced, are well known for the hydrides of rare-earth metals (see, for example, Ref. 61) and can be explained by the presence of an effective negative charge on the hydrogen atoms in these hydrides; this charge is produced by the removal of some valence electrons of the metal atoms from the conduction band and localization of these electrons on the hydrogen atoms. From this standpoint, as the content of H(D, T) in the hydride MeH_c increases, its metallic properties, for example, its electric conductivity, should be diminished and, conversely, the properties corresponding to the ionic compound $Me^+H_c^-$ should be enhanced. This effect is indeed observed, for example, in the series of lanthanum hydrides $LaH_2 \rightarrow LaH_{2.3-3.0}$, which, like PdH and TiH_2, has an fcc lattice. As the concentration increases from $C = 2$ up to $C = 3$ the conductivity of the hydride LaH_c decreases by approximately a factor of 100 and the phase with the maximum concentration approaches the ionic compound $La^{+++}H_3^-$. When the hydride LaH_2 is formed all tetrahedral voids are filled, and when the trihydride is formed the octahedral voids are filled, right up to the composition LaH_3. An analogous behavior is also exhibited by hydrides of other rare-earth metals, where the first hydride MeH_2 is characterized by metallic conduction (metallic hydride) and the more highly saturated hydride MeH_3 is a semiconductor (ionic or ionic-covalent hydride).

Can an analogous enhancement of the dielectric properties be expected for transition-metal hydrides when the concentration of H(D, T) in them increases? To answer this question, we shall examine in greater detail the coordination of hydrogen atoms in a metal. As we have already mentioned above, the fcc and hcp structures typical for metals contain one octahedral and two tetrahedral voids per metal atom, while a bcc lattice contains three and six voids, respectively, per metal atom. From a geometrical criterion, based on the consideration of stability of the packing of hard spheres, it should be expected that for hydrides octahedral coordination is advantageous for $0.41 \leqslant R_H/R_{Me} \leqslant 0.73$ and tetrahedral coordination is favored for $0.22 \leqslant R_H/R_{Me} \leqslant 0.41$.[61] For transition metals the ratio R_H/R_{Me} falls in the range 0.22–0.41, and hydrogen atoms in hcp and fcc metals should occupy tetrahedral positions. In most cases this does in fact happen, but, for example, in Ni and Pd, in contradistinction to what was said above, hydrogen occupies octahedral voids.

Analysis of data on transition-metal hydrides[61] points to a definite regularity in the change in the coordination of hydrogen (of the type of interstices) as a function of the radius of the metal atoms. For small atoms octahedral coordination is characteristic, while for large atoms tetrahedral coordination is characteristic, with the coordination changing at $R_{Me} = 1.34$–1.37 Å.

It is important to emphasize that this behavior pertains precisely to stable hydrides, which can exist after the conditions for nonequilibrium saturation are no longer satisfied.

In order for such hydrides to form, the voids cannot be too small so that hydrogen atoms could occupy them, but they also should not be too large—otherwise the hydrogen will escape from them after the conditions of nonequilibrium saturation are no longer satisfied.

In the light of the considerations presented above, it is natural to conjecture that under the conditions of nonequilibrium saturation in a layer near the surface, through which H(D, T) penetrates into the metal, unstable phases with high concentration of H(D, T), possibly, right up to the maximum concentration for a lattice of a given type or a modification of it, can form. This, in turn, can result in enhancement of the dielectric properties in the unstable phase either as a result of the removal of some of the electrons from the conduction band (as for hydrides of rare-earth elements) or owing to the expansion of the crystal lattice.

Consider, for example, the γ' phase of TiH_2 with the highest hydrogen concentration. It has an fcc lattice with tetrahedral voids, occupied by H atoms. An estimate of the sizes of the octahedral voids gives

$$R_0^{TiH_2} = 0.5\,(a_{\gamma'} - 2R_{Ti}) \approx 0.77\text{Å},$$

which is much greater than the size of the hydrogen atom ($R^H \approx 0.53$ Å). This means that in the hypothetical (unstable) phase TiH_3 the excess hydrogen atoms can remove some of the electrons from the conduction band, and this should enhance the dielectric properties. (The electronegativities of H and Ti are $\chi_H = 2.1$ and $\chi_{Ti} = 1.5$.)

The situation is different for palladium hydride. Since $\chi_{Pd} = 2.2$ is higher than χ_H, in this case hydrogen is now a donor and gives up its electrons to the Pd atoms. Recent cluster-model calculations, performed by Sun and Tomanek,[88] have indeed shown that the assumptions made in Ref. 8 is confirmed, and that on saturation to the state PdH_2 palladium hydride goes over into a semimetallic state. It should be noted, however, that the closeness of the electronegativities of Pd (2.2) and H (2.1) can make this effect quite weak. It is possible that in the case of Pd the main mechanism of the enhancement of the nonmetallic properties is connected with the expansion of the crystal lattice.

For palladium hydride, in which the octahedral positions are filled ($R_0^{PdH} = 0.5(a_\beta - 2R_{Pd}) \approx 0.705$ Å), the increase in concentration owing to filling of the remaining unfilled tetrahedral positions by individual deuterons or octahedral positions by DD pairs can result in either restructuring or strong deformation of the lattice (and subsequent fracture).

In this respect the results of Ref. 121 are of great interest. In Ref. 121 a new palladium hydride, having the chemical composition $PdH_{1.33}$, was discovered. It was found that this hydride has a tetragonal lattice with cell parameters $a = 2.896$ Å and $c = 3.330$ Å. A remarkable feature of this phase is that hydrogen is distributed in an ordered fashion in the tetrahedral voids of the body-centered lattice and, at the same time, the metallic lattice contains an enormous number of vacancies (25% or $2 \cdot 10^{22}$ cm^{-3}). The phase found is stabilized with the help of very rapid deposition of a thin palladium film ($\sim 10^3$ Å), saturated with hydrogen from the gas phase at high temperature, or by the method of ion implantation.

It is obvious that the existence of such a large number of statistically distributed vacancies should result in a sharp reduction of the electric conductivity of this phase.

Another factor, which in the general case can reduce the electric conductivity and the associated discharging of the "microcapacitors" through the surrounding hydride mass, is connected with the character of the fracturing, to which the surface layer of the hydride is subjected. It is well known that this fracturing can result in the formation of a "hydride sponge" and subsequent fragmentation of the surface layer. As a result the surface layer of the material becomes discontinuous, and this sharply reduces the electric contact between the separate particles into which the surface layer decomposes.

With regard to the expansion of the crystal lattice of the hydride phase, it is known that it increases approximately linearly as a function of the concentration. It can be expected that at the high concentrations characteristic for unstable phases the deformation becomes very large; this ultimately results in fracturing of the hydride layer. At the same time, as is well known from the band theory of solids (see, for example, Ref. 122), the increase in the interatomic distance in the crystal should result in narrowing of the allowed bands and broadening of the forbidden bands. This means that, in the general case, it can be expected that for unstable phases with high H(D) concentration the dielectric properties of the material will be enhanced.

In concluding this section we stress that the foregoing analysis does not prove that the dielectric properties are enhanced in the unstable hydride phase of transition metals. However, based on the hypothesis that the nuclei overcome the Coulomb barrier as a result of being accelerated in local electric fields in the microcracks, it is necessary to make the additional (and very strong) assumption that the properties of the disintegrating deuteride are close to those of an ionic crystal. (We note, in passing, that in application to fusion of this type the term cold is very arbitrary. It merely reflects the fact that the crystal in which the reaction occurs is at room temperature, while the energy of the deuterium ions penetrating into it is low (eV). As regards the microscopic conditions for fusion of accelerated deuterons, they, of course, correspond to high effective temperatures $\sim 10^7$ K.)

I wish to make two additional remarks.

1) In Ref. 116 the appearance of excess charges accompanying cracking of hydrides is attributed to the expansion of the crystal lattice, as a result of which different surface charge density can arise at the boundary between phases with different H concentration. In the case of a metallic bond, however, the fact that charges appear on the surface is itself not explained.

2) In Refs. 51 and 74 the cold-fusion phenomenon is thought to be associated with neutron emission, observed in Ref. 9, accompanying mechanical fracture of (ionic) LiD crystals. It is conjectured that in the course of electrolysis, when LiOD is present in the electrolyte, regions containing LiD form in the electrode. Cracking of the hydride results in fracture of LiD and neutron emission. This explanation, however, is hardly correct for electrolysis, because it presumes that Li is strongly dissolved in the metal (this is not confirmed experimentally) and is not applicable at all to experiments in which Li is not employed, for example, when metals are saturated with deuterium from the gas phase.

4.2. Acceleration mechanism under conditions of cracking

As we have already pointed out, the mechanoemission of electromagnetic waves accompanying fracture is usually interpreted with the help of the idea that charges arise on the sides of the cracks and generate a strong field.

We shall give some estimates for the simplest model, in which a crack is regarded as a flat capacitor with area $\sim l^2$ and gap $d = 0.1l$.

Since the lattice constant of hydrides is typically equal to 3–4 Å, we obtain the following estimate for the maximum surface charge density:

$$\Sigma \sim \frac{e}{a^2} \sim e \cdot 10^{15}\,\text{cm}^{-2} = eJ,$$

where J is the density of hydrogen or deuterium ions. In many cases, because some ions are neutralized at the surface the charge density can be greatly reduced; thus, in Ref. 10 the estimate $J \sim 10^{10}$–10^{14} cm^{-2} is given for adhesion layers.

The electric field in such a capacitor is $E \sim \Sigma \sim 10^8$ V/cm, and the potential difference with $d \sim 10^{-5}$–10^{-4} cm is $U \sim Ed \sim 10^3$–10^4 V. Therefore, in such a capacitor an ion can acquire energy $W \sim 1$–10 keV.

However acceleration up to such energies will occur only if the time required for acceleration $t_{\text{acc}} \sim d(m_{\text{D}}/W)^{1/2} \sim (0.7\text{–}2)\,10^{-12}$ s is much shorter than the lifetime of the charge on the capacitor. The time over which the capacitor is discharged through the surrounding matter depends on the resistance and structure of this matter. If it is assumed that the resistivity of the hydride is close to metallic resistivity, then $t_{\text{frac}} \leqslant 10^{-15}$ s $< t_{\text{acc}}$.[8] For this reason, in order that the discharge through the hydride be insignificant, either the hydride must be strongly fragmented or conduction of nonmetallic type must arise in the hydride.

The second possible reason for discharging is electron field-emission. In order that electron field-emission not impede the acceleration of deuterium ions, the condition that the hydride transform into a dielectric state is also significant, since in this case the field-emission time $t_{\text{f.e}} \sim \Sigma/j_{\text{f.e}} \sim 10^{-10}$ s $> t_{\text{acc}}$, where $j_{\text{f.e}} \sim 10^6$ A·cm^{-2} is the density of the field-emission current from dielectrics.[123] For metals $t_{\text{f.e}}$ is several orders of magnitude lower.[6)]

Therefore, in order for the acceleration mechanism of cold fusion to be efficient it is critically important that the conditions discussed in Sec. 4.1 be satisfied, i.e., the dielectric properties of the hydride must be enhanced or the hydride must be fragmented; this results in significant degradation of the electric contact between separate charged parts of microcracks, so that $t_{\text{acc}} < t_{\text{frac}}^{(\text{eff})}$.

In order to estimate the neutron yield we shall assume that cold fusion occurs by means of the fusion of deuterium ions accelerated in this manner with the deuterium ions on the opposite side of a crack; the effective thickness of this layer is determined by the range of deuterium ions at which a fusion reaction is still possible.

We shall first study the least favorable situation, in which the target consists of a single layer of deuterium atoms on the surface of a crack, and the cross section for DD fusion is determined by the fusion of "bare" deuterium nuclei neglecting screening effects. Assuming that the surface density of deuterium in the target is equal to J, we obtain for the number of neutrons from a single "accelerator" crack

$$N^{(1)} \sim J^2 l^2 \sigma(W),$$

where σ is the cross section for the reaction $\text{D} + \text{D} \rightarrow {}^3\text{He} + \text{n}$. In the region $W \sim 1$–10 keV the cross section σ grows very rapidly with W; for estimates, we shall use the characteristic value $\sigma \sim 10^{-32}$ cm^2.[7)] Assuming that $\Delta V/V = 0.1$ and $n_{\text{T}} \sim 10^{12}$–$10^9$ cm^{-3} we obtain the following estimate of the neutron yield of a unit volume of material that has absorbed hydrogen:

$$n_{\text{n}} \sim N^{(1)} n_{\text{T}} \sim 10^2 - 10\,\text{cm}^{-3}.$$

This estimate can be compared with the experimental results of Ref. 6. For an electrode density of $\sim 10^{22}$ Ti atoms/cm^3 and hydrogen-absorption time $\sim 10^4$ s (several hours) we obtain $n_n^{(\text{exp})} \sim 10^3$ neutrons/cm^3. A neutron yield of the same order of magnitude was obtained in the experiment of Ref. 9, in which about 10 neutrons were observed to accompany fracture of a LiD crystal with a volume of 0.04 cm^3, i.e., $n_{\text{n}}^{\text{exp}} \sim 250$ neutrons/cm^3.

In the more general form

$$n_{\text{n}} \approx J_{\text{acc}} J_{\text{tar}} \frac{\delta}{a_0} \frac{\Delta V}{V} d^{-1}\sigma \quad (W \approx 4\pi e^2 J d),$$

where J_{acc}, J_{tar}, and J are the surface densities of the accelerated ions, the target atoms, and the charges generating the accelerating field. Taking into account the range of deuterons in the material $\delta/a_0 \sim E_{\text{D}}/\Delta E \sim 10^2$–$10^4$, as well as the energy dependence of the DD fusion cross section $\sigma(C) \sim \sigma(l)$ can increase the above estimate by several orders of magnitude and thereby explain the experimentally observed strong neutron bursts.[7)]

We stress once again that in the acceleration model cold fusion is regarded as "microscopically hot" fusion, in which the Coulomb barrier is overcome owing to the energy stored in the hydride. It is entirely possible that, together with this, other effects, such as screening, which should also be included in this case in scenarios of cold fusion, should play an important role in cold-fusion processes. We note that the predominant formation of tritium, as observed in Ref. 17, cannot be explained on the basis of a purely acceleration mechanism.

4.3. Conclusions for experiments

The assumptions on which the acceleration model is based and the conclusions following from this model can be directly checked experimentally. We shall once again formulate the basic assumptions.

a) When nonequilibrium saturation of transition metals with hydrogen (D, T) occurs unstable hydride phases with a high concentration of hydrogen, higher than in the stable phases, can arise.

b) The properties of hydrides in these phase states can be close to those of dielectrics or semiconductors.

c) The expansion of the crystal lattice and the concentration-induced stresses and embrittlement, which accompany the growth of the hydride layer, result in fracture of the hydride and its saturation with a network of microcracks.

d) The appearance of cracks is accompanied by the appearance of electric charges. The fields generated by these charges can accelerate deuterium ions and initiate cold-fusion reactions with adequate efficiency. From here there follow a number of conclusions and predictions.

1. Cold fusion is primarily of a surface process, i.e., it develops in the surface layer of the hydride, which in this time interval is subject to fracture. As the process progresses deeper into the material it encompasses new layers of the hydride.

2. Nonequilibrium conditions of saturation of the metal with deuterium or desorption are important for the process to proceed.

3. To create favorable conditions it is necessary to use metals that are capable of dissolving large quantities of deuterium (hydrogen). (Owing to the extensive development of hydrogen-storage technology a large number of such metals and alloys are now known.)

4. The conditions of saturation must provide an adequate concentration gradient, capable of generating internal concentration stresses which locally exceed the fracture stress of the material.

5. The hydride formed should have a low plasticity.

6. The temperature and rate of saturation must be chosen so as to eliminate any effects due to stress relaxation.

7. Since the fracture of the hydride occurs in a stochastic manner with some possible quasiperiodic modulation in time the cold-fusion reactions proceed in an analogous manner.

Based on the foregoing conclusions we can make quite obvious recommendations in order to check the proposed mechanism experimentally.

a) Since an important part of the model is the assumption that there exist unstable phases with a high concentration of hydrogen, it is important to analyze the structure and composition *in situ*, i.e., directly in the course of nonequilibrium absorption of hydrogen. This can be done, in particular, by means of x-ray structural analysis, neutron-diffraction analysis, and electron-microscopic analysis of the surface and surface layer.

b) Information about the enhancement of dielectric properties in the unstable phase can be obtained from measurements of the electrical conductivity (also *in situ*). Such measurements are obviously best performed with the help of thin films, whose thickness is close, in order of magnitude, to the characteristic critical (for fracture) thickness of the hydride layer ($\sim 10^3$–10^5 Å). Another possibility is to use hydrides in which the bonding is known to be ionic or varies with the concentration, as in the case of hydrides of rare-earth metals.

c) The conjecture that cold-fusion reactions are connected with the appearance of cracks can be checked by studying the correlation between the detected products of cold fusion (neutrons and protons) and the acoustic emission generated when cracks form. Another possibility is to study the correlations with initiation of crack formation, for example, with the help of mechanical strains, ultrasonic pulses, thermal, cryogenic, and electric shocks, etc.[7,8]

d) The role of acceleration in electric fields can be studied with the help of correlations of the products of cold fusion and the electromagnetic emission at different wavelengths.[7,8]

Obvious recommendations can also be made for checking the consequences 1–7) given above:

1) The surface character of the phenomenon can be checked by comparing results for samples with different surface to volume ratios.

2) The great importance of nonequilibrium saturation can be checked by varying the experimental conditions. The items 3–6) can also be easily checked by changing the experimental conditions and the materials employed. We note that different metals and alloys can have a very different susceptibility to hydrogen-induced fracture and this makes it possible to vary this property of a material over wide limits.

7) Finally, the stochastic and quasiperiodic nature[7,8] of the cold-fusion signals has actually already been confirmed in the analysis of events as a function of time with narrow time bins.

CONCLUSIONS

We shall now summarize our discussion and formulate the main results.

1. Evidence for the existence of cold-fusion phenomena, i.e., the appearance of reactions in which deuterons, injected into the crystal lattice of metals, fuse at room temperature, has been obtained in a number of experimental investigations.

2. The rates and character of cold-fusion reactions can be different. The reactions can be manifested either in the form of chaotic emission of single neutrons, which can continue for several hours at an average rate of $\Lambda \sim 10^{-24}$–10^{-22} s^{-1} $(DD)^{-1}$ or in the form of separate "neutron bursts," in which up to 10^3–10^5 neutrons can be emitted in short time intervals (seconds, minutes). The emission induced by the charged products of DD fusion (p, T, ^{3}He) has also been recorded.

3. The characteristic features of experiments on cold fusion are that the results are not consistently reproducible, the signals are sporadic, and signals appear only if nonequilibrium conditions are created in the metal-deuterium system.

4. In spite of the significant efforts made by many tens of scientific groups throughout the world cold-fusion has been studied only at the "preliminary," qualitative level. Many results require further checking. This primarily concerns the question of the relationship of different channels and the possibility that cold fusion occurs with a high rate primarily in the neutron-free channel ($n/T \sim 10^{-8}$).[17] More detailed experiments on the direct detection of charged particles and the study of fusion in pD and DT systems as well as correlation experiments in several detection channels must be performed, and the effect of different factors on the character of the flow of cold-fusion processes must be investigated.

5. At the present time there is no generally accepted viewpoint regarding the mechanism of cold fusion. The experimentally observed results cannot be explained on the basis of the standard ideas of nuclear physics and solid-state physics for equilibrium systems. The most promising model is apparently the acceleration model, in which it is posited that cold fusion is brought about by the acceleration of deuterons in strong electric fields generated in microcracks. Actually, "microscopically hot fusion" ($T_{eqv} \sim 10^7$ K) rather than "cold fusion" occurs. The sporadic character of cold fusion, the observation of "neutron bursts," and in many cases the quasiperiodicity of the bursts and the absence of the 5.5 MeV γ-ray line (see footnote 2) are the evidence for such a model. More definitive evaluations, however, require correlation experiments (see footnote 3), in which the "associated" signals (radio and acoustic emission, etc.)[8] are de-

tected, and detailed theoretical calculations, in which different solid-state effects (screening, enhancement of dielectric properties, etc.) are taken into account, must be performed.

6. The energy released in cold-fusion reactions corresponding to the observed neutron fluxes is too low to be of interest from the standpoint of the production of electricity. The situation could become more interesting, if the possibility of a substantially higher rate of cold fusion in the neutron-free channel is confirmed. Irrespective of this, the study of cold fusion is certainly of interest for a number of disciplines, such as solid-state physics, geophysics, geochemistry, radiation chemistry, radiation acoustics, etc.

I thank D. A. Kirzhnits for his interest in this work and for support and P. I. Golubnichiĭ, G. I. Merzon, G. A. Tsirlina, V. A. Chechin, and the participants of the seminars at the Physics Institute of the Academy of Sciences, the Joint Institute of Nuclear Research, the Institute of Atomic Energy, the Institute of High-Energy Physics, the Institute of Theoretical and Experimental Physics, and the Winter School of 1990 on Physics in Bakuriani for many helpful discussions.

[1)] After this review was written, there appeared new studies[124,125] in which it is likewise reported that neutron bursts were observed to accompany electrolytic saturation of palladium with deuterium.

[2)] Further evidence for hot fusion is provided by the results of Ref. 126, where it is shown that in the process of electrolysis with D_2O and a tritium-saturated titanium cathode the rate of the cold-fusion reaction $T + D \rightarrow {}^4He(3.5\ MeV) + n(14.1\ MeV)$ is approximately two orders of magnitude higher than that found in Ref. 6 for DD fusion.

[3)] P. I. Golubnichiĭ *et al.*[127] recently reported that, using palladium electrolytically saturated with deuterium, over an observational period of 11 h they recorded two events with strong (within 10 μs) correlation of nuclear, acoustic, and radio emissions and they measured the amplitudes of the acoustic and radio signals. The expected number of random triple coincidences over the measurement time was equal to 10^{-7} events.

[4)] Negative results on muonic catalysis of cold fusion were likewise obtained with deuterated palladium and titanium samples irradiated in an accelerator with a beam of 1.9–3.0 MeV muons.[128]

[5)] See also the recent work of S. E. Segre *et al.*[129] In addition, I also learned that the possibility of the acceleration mechanism of cold fusion was also mentioned by S. S. Gershteĭn and L. I. Ponomarev at a conference on cold fusion in Erice (Italy) in April 1989.

[6)] Electron field-emission can also be suppressed owing to the properties of the juvenile surface of a crack. In this connection we recall that appropriately treated surfaces of metallic resonators in accelerators can withstand fields of up to 10^8 V/cm without the appearance of an appreciable field-emission current.

[7)] More accurate estimates, taking into account the energy dependence $\sigma_{muc}(E) \sim \sigma_{muc}(I)$, are presented in Ref. 130.

[8)] In Ref. 130 it is shown that mutual consistency between the number of events recorded in Ref. 127 and the measured pulse amplitudes can be achieved on the basis of the acceleration model. It should be kept in mind, however, that none of the current evidence supporting the acceleration model in microcracks can be regarded as unequivocal confirmation of the model. This is primarily because the evidence admits an alternative interpretation. Thus the fracture of hydride under the conditions of nonequilibrium in the metal-hydrogen system can be only an associated phenomenon and not the reason for cold fusion. In exactly the same way hot fusion need not occur in cracks, but, for example, result from acceleration in electric fields of the surface layer. In addition, it should not be forgotten that the indicated observations are of a preliminary character and must be checked further. Nonetheless the fact that all observations are consistent with the acceleration model cannot be ignored. In this connection it is also of interest to check other predictions of the acceleration model.[7,8]

P. I. Golubnichniĭ *et al.*[131] recently reported on measurements performed in the low-background laboratory of the Baksan Neutrino Observatory of the Institute of Nuclear Research of the Academy of Sciences of the USSR. Forty-two events were recorded in which neutrons were emitted and which were correlated with acoustic pulses (the expected number of random coincidences was ~6).

[1]M. D. Lemonick, *Time*, May 8, 1989, p. 72.
[2]S. Begley, H. Hurt, and A. Murr, *Newsweek*, May 8, 1989, p. 41.
[3]R. N. Kuz'min and B. N. Shvilkin, Cold Fusion [in Russian], Znanie, M., 1989, Ser. Fizika, No. 10.
[4]V. A. Tsarev, Nauka i zhizn', No. 3, 18 (1990).
[5]M. Fleischmann and S. Pons, J. Electroanal. Chem. **261**, 301 (1989); Erratum, *ibid.* **263**, 187 (1989).
[6]S. E. Jones, E. P. Palmer, J. B. Czirr *et al.*, Nature (London) **338**, 737 (1989).
[7]P. I. Golubnichiĭ, V. A. Kurakin, A. D. Filonenko *et al.*, Preprint No. 113, Physics Institute of the Academy of Sciences of the USSR, Moscow, April, 1989; Dokl. Akad. Nauk SSSR **307**, 99 (1989) [Sov. Phys. Dokl. **34**(7), 628 (1989)].
[8]P. I. Golubnichiĭ, V. A. Tsarev, and V. A. Chechin, Preprint No. 149, Physics Institute of the Academy of Sciences of the USSR, Moscow, July, 1989.
[9]V. A. Klyuev, A. G. Lipson, Yu. P. Topornov *et al.*, Pis'ma Zh. Tekh. Fiz. **12**, 1333 (1986) [Sov. Tech. Phys. Lett. **12**, 551 (1986)].
[10]B. V. Deryagin, N. A. Krotova, and V. P. Smilga, *Adhesion of Solids* [in Russian], Nauka, M., 1973.
[11]*Abstracts of Reports at the 10th Anniversary All-Union Symposium on Mechanoemission and Mechanochemistry of Solids* [in Russian], September 24–26, 1986, Rostov-na-Donu, Moscow, 1986.
[12]A. Bertin, M. Bruschi, M. Capponi *et al.*, Nuovo Cimento A **101**, 997 (1989).
[13]F. Celani, M. de Felice, E. L. Fabbri *et al.*, Frascati Preprint LNF-89/048 (1989) (submitted to Nuovo Cimento).
[14]V. D. Rusov, T. N. Zelentsova, N. Yu. Semenov *et al.*, Pis'ma Zh. Tekh. Fiz. **15**, No. 9, 90 (1989) [Sov. Tech. Phys. Lett. **15**, 743 (1989)].
[15]A. de Ninno, A. Frattolillo, G. Lollobattista *et al.*, Nuovo Cimento **101**, 841 (1989).
[16]H. O. Menlove, M. M. Fowler, E. Garcia *et al.*, LANL Report LA-VR-89-1570 (1989).
[17]a) P. K. Iyengar, Paper Submitted to the 5th International Conference on Emerging Nuclear Energy Systems (ICENES V), Karlsruhe, FRG, July 3–6, 1989. b) P. K. Iyengar and M. Srinivasan [Eds.], BARC Studies in Solid Fusion, BARC-1500, Bhabha Atomic Research Centre, Bombay, 1989.
[18]A. T. Budnikov, V. M. Zuber, G. A. Kartamyshev *et al.*, Preprint IMK-89-4, Khar'kov (1989).
[19]I. A. Borovoĭ,A. T. Budnikov, E. L. Vinograd *et al.*, Preprint IMK-89-5, Khar'kov, 1989.
[20]D. Abriola, E. Achtenberg, M. Davidson *et al.*, J. Electroanal. Chem. **265**, 355 (1989).
[21]D. Secliger, K. Wiesener, A. Meister *et al.*, Electrochim. Acta **34**, 991 (1989).
[22]I. A. Borovoĭ,E. L. Vinograd, N. Z. Golunov *et al.*, Preprint IMK-89-9, Khar'kov, 1989.
[23]J. Zak and J. W. Strojek, Papers Submitted to the 40th Meeting of the International Society of Electrochemistry, Kyoto, 1989, Vol. 2, p. 1335.
[24]T. Mizuno, T. Akimoto, and N. Sato, *ibid.*, p. 1333.
[25]J. O'M. Bockris, K. Wolf, R. Kainthla *et al.*, *ibid.*, p. 1332.
[26]V. F. Zelenskiĭ, V. F. Rybalko, A. N. Morozov *et al.*, Preprint 89-61, Khar'kov Physicotechnical Institute, Khar'kov, 1989.
[27]V. B. Brudanin, V. M. Bystritskiĭ, V. G. Egorov *et al.*, Preprint D15-89-347 (In Russian), Joint Institute for Nuclear Research, Dubna, 1989.
[28]G. Kreysa, G. Marx, and W. Plieth, J. Electroanal. Chem. **266**, 437 (1989).
[29]E. Buchanan, R. Hirosky, J. Jorne *et al.*, Preprint ER 13065-578, 1989.
[30]A. Baurichter, W. Eyrich, M. Frank *et al.*, Z. Phys. B **76**, 1 (1989).
[31]D. Alber, O. Boebel, C. Schwarz *et al.*, Z. Phys. A **333**, 319 (1989).
[32]S. Blagus, M. Bogovac, D. Hodko *et al.*, Z. Phys. A **333**, 321 (1989).
[33]J. P. Blaser, O. Haas, C. Petitjean *et al.*, Preprint PSI-PR, 89-17, Villigen, Switzerland, 1989.
[34]S. Baba, K. Kawamura, and N. Taniguchi in Ref. 23, p. 1341.
[35]N. Oyama, T. Ohsaka, O. Hatozaki *et al.*, *ibid.*, p. 1336.
[36]V. B. Brudanin, V. M. Bystritskiĭ, V. G. Egorov *et al.*, Preprint D 15-89-314 (In Russian), Joint Institute for Nuclear Research, Dubna, 1989.
[37]M. Gai, S. L. Rugari, R. H. France *et al.*, Nature (London) **340**, 29 (1989).
[38]N. S. Lewis, C. A. Barnes, M. J. Heben *et al.*, Nature (London) **340**, 525 (1989).
[39]A. Kira, S. Nakabayashi, S. Yamagita *et al.* in Ref. 23, p. 1339.
[40]R. Aleksan, M. Avenier, G. Bagien *et al.*, Preprint DPhPE 89-19, LPC-89-17, CEN, Saclay, France, 1989.
[41]R. D. Petrasso, X. Chen, K. W. Wenzel *et al.*, Nature (London) **339**, 183 (1989).
[42]M. Fleischmann, S. Pons, and R. J. Hoffman, Nature (London) **339**, 667 (1989).

[43]R. D. Petrasso, X. Chen, K. W. Wenzel *et al.*, Nature (London) **339**, 667 (1989).
[44]G. Chrider, H. Wipf, and A. Richter, Z. Phys. B **76**, 141 (1989).
[45]R. Behrisch, W. Holler, J. Roth *et al.*, Nucl. Fusion **29**, 1187 (1989).
[46]S. M. Bennington, R. S. Sokhl, P. R. Stonadge *et al.*, Electrochim. Acta **34**, 1323 (1989).
[47]H. Uchida, Y. Matsumura, J. Hayashi *et al.* in Ref. 23, p. 1346.
[48]A. A. Kosyachkov, V. S. Triletskiĭ, V. T. Cherepin *et al.*, Pis'ma Zh. Eksp. Teor. Fiz. **49**, 648 (1989) [JETP Lett. **49**(12), 744 (1989)].
[49]R. Kainthla, O. Velev, L. Kaba *et al.*, Electrochim. Acta **34**, 1315 (1989).
[50]R. Huggins and M. Scherber, *Proceedings of the Cold Fusion Workshop, Santa Fe, May 25-28, 1989*. A. J. Appleby and S. Srinivasan, *ibid.* U. Landau, Meeting of Electrochemistry Society, Los Angeles, 1989.
[51]J. W. Schultze, U. Konig, A. Hochfeld *et al.*, Electrochim. Acta **34**, 1289 (1989).
[52]M. Keddam, *ibid.*, p. 995.
[53]V. A. Shapovalov, Pis'ma Zh. Eksp. Teor. Fiz. **50**, 109 (1989) [JETP Lett. **50**(3), 117 (1989)].
[54]R. D. Armstrong, E. A. Charles, I. Fells *et al.*, Electrochim. Acta **34**, 1319 (1989).
[55]M. A. Yaroslavskii, Dokl. Akad. Nauk SSSR **307**, 369 (1989); *ibid.* **307**, 600 (1989) [Sov. Phys. Dokl. **34**(7), 637 (1989); *ibid.*, 648 (1989)].
[56]A. G. Lipson, D. M. Sakov, V. A. Klyuev *et al.*, Pis'ma Zh. Eksp. Teor. Fiz. **49**, 588 (1989) [JETP Lett. **49**, 675 (1989)].
[57]A. G. Lipson, V. A. Klyuev, B. V. Deryagin *et al.*, Pis'ma Zh. Tekh. Fiz. **15**, No. 10, 88 (1989) [Sov. Tech. Phys. Lett. **15**, 783 (1989)].
[58]V. I. Mikheeva, *Transition-Metal Hydrides* [in Russian], USSR Academy of Sciences Press, Moscow, 1960.
[59]E. G. Maksimov and O. A. Pankratov, Usp. Fiz. Nauk **116**, 385 (1975) [Sov. Phys. Usp. **18**(7), 481 (1976)].
[60]V. I. Mikheeva, Izv. Akad. Nauk SSSR, Neorg. Mater. **14**, 1558 (1978).
[61]Yu. Z. Nozik, R. P. Ozerov, and K. Khennig, *Structural Neutron Diffraction Analysis* [in Russian], Atomizdat, M., 1979, Vol. 1.
[62]G. Alefeld and I. Volkl, (Eds.) *Hydrogen in Metals*, Springer-Verlag, N. Y., 1978, Vols. 1 and 2 [Russ. transl., Mir, M., 1981].
[63]I. Ya. Dekhtyar and V. I. Shevchenko, Phys. Status Solidi **49**, 11 (1972).
[64]T. Graham, Phil. Trans. Roy Soc. **156**, 399 (1866).
[65]V. M. Katlinskii, Izv. Akad. Nauk SSSR, Neorg. Mater. **14**, 1667 (1978).
[66]V. N. Lobko and R. A. Ryabov, "Diffusion of hydrogen in metals under the conditions of growth of a hydride layer," Dep. No. 818-D83 [in Russian], Polytechnical Institute, Vladimir (1983).
[67]L. G. Malyshev, S. A. Lebedev, R. A. Ryabov *et al.*, Izv. Vyssh. Uchebn. Zaved., Fiz., No. 3, 43 (1982) [Sov. Phys. J. (1982)].
[68]O. B. Khavroshkin, B. A. Tsarev, V. V. Tsyplakov *et al.*, Kr. soobshch. fiz., FIAN SSSR, No. 5, 60 (1985); *ibid.*, No. 10, 26 (1985) [Sov. Phys. Lebedev Inst. Rep. (1985)].
[69]P. I. Golubnichiĭ and A. D. Filonenko, Izv. Akad. Nauk SSSR, Ser. Fiz. **53**, 366 (1988) [Bull. Akad. Sci. USSR, Phys. Ser. (1988)].
[70]V. V. Panasyuk *et al.*, Fiz.-khim. mekh. materialov, No. 3, 3 (1984).
[71]V. A. Gol'tsov, A. F. Volkov, E. I. Grinchenko *et al.*, Preprint, (In Russian) Donetsk Polytechnical Institute, Donetsk, 1984.
[72]S. E. Koonin and M. Nauenberg, Nature (London) **339**, 690 (1989).
[73]I. K. Kikoin [Ed.], *Handbook of Tables of Physical Quantities* [in Russian], Atomizdat, M., 1976.
[74]J. S. Cohen and J. D. Davies, Nature (London) **338**, 705 (1989).
[75]C. J. Horowitz, Phys. Rev. C **40**, 1555 (1990).
[76]J. Rafelski, M. Gajda, D. Harley *et al.*, Preprint AZPH-TH/89-19, Tucson (1989).
[77]V. I. Vysotskiĭ and R. N. Kuz'min, Pis'ma Zh. Tekh. Fiz. **7**, 981 (1981) [Sov. Tech. Phys. Lett. **7**, 422 (1981)].
[78]V. I. Vysotskiĭ and R. N. Kuz'min, Zh. Tekh. Fiz. **53**, 1861 (1983) [Sov. Phys. Tech. Phys. **28**, 1144 (1983)].
[79]S. E. Koonin, Preprint, Univ. of California, Santa Barbara (1989).
[80]W. Kolos and L. Wolniewicz, J. Chem. Phys. **41**, 3663 (1964); *ibid.* **49**, 404 (1968).
[81]W. Byers-Brown and J. D. Power, Proc. R. Soc. London A **317**, 545 (1970).
[82]K. Langanke, H. J. Assenbaum, and C. Rolfs, Z. Phys. A **333**, 317 (1989).
[83]Ya. B. Zel'dovich and S. S. Gershteĭn, Usp. Fiz. Nauk **71**, 581 (1960) [Sov. Phys. Usp. **3**(4), 593 (1961)].
[84]C. D. van Siclen and S. E. Jones, J. Phys. G **12**, 213 (1986).
[85]J. Kondo, J. Phys. Soc. Jpn. **58**, 1869 (1989).
[86]L. L. Lohr, J. Phys. Chem. **93**, 4697 (1989).
[87]E. A. Stern, Preprint, Univ. of Washington, Seattle (1989).
[88]Z. Sun and D. Tomanek, Phys. Rev. Lett. **63**, 59 (1989).
[89]A. J. Leggett and G. Baym, Nature **340**, 45 (1989).
[90]E. Wicke, H. Brodowsky, and B. Brodowsky, *Hydrogen in Metals II*, Springer-Verlag, New York (1978) (Topics in Applied Physics, **Vol.** 29).
[91]T. Garel, J. C. Niel, and H. Orland, Preprint PhT/89-87, CEN, Saclay France (1989).
[92]C. Walling and J. Simons, J. Phys. Chem. **93**, 4693 (1989).
[93]T. Tajima, H. Iyetomi, and S. Ichimaru, Preprint DOE/ET-53088-369, UFSR No. 369, Austin (1989).
[94]A. S. Davydov, Ukr. Fiz. Zh. **34**, 1295 (1989).
[95]A. J. McCevoy and C. T. D. O'Sullivan, Nature **338**, 711 (1989).
[96]F. C. Frank, Nature **160**, 525 (1947).
[97]A. D. Sakharov, Otchet FIAN SSSR, Moscow (1948).
[98]Ya. B. Zel'dovich, Dokl. Akad. Nauk SSSR **95**, 454 (1954).
[99]Ya. B. Zel'dovich and A. D. Sakharov, Zh. Eksp. Teor. Fiz. **32**, 947 (1957) [Sov. Phys. JETP **5**, 775 (1957)].
[100]S. S. Gershteĭn and L. I. Ponomarev in: Muon Physics, edited by V. Hughes and C. S. Wu, Academic Press, N. Y., 1975, Vol. 3, p. 141.
[101]G. Zweig, Science **201**, 973 (1978).
[102]R. Cahn, Phys. Rev. Lett. **40**, 80 (1978).
[103]P. Freund and C. Hill, Nature **276**, 250 (1978).
[104]B. L. Ioffe, L. B. Okun, M. A. Shifman *et al.*, Acta Phys. Polon. B **12**, 229 (1981).
[105]G. L. Shaw, R. W. Bland, L. Fonda *et al.*, Preprint, Univ. of California, Irvine, 1989.
[106]P. Paolo, Nature (London) **338**, 711 (1989).
[107]V. I. Goldanskiĭand F. I. Dalidchik, Nature (London) **342**, 231.
[108]I. R. Oppenheimer and M. Phillips, Phys. Rev. **48**, 500 (1935).
[109]A. A. Shihab-Elden, J. O. Rasmussen, M. Justice *et al.*, Preprint LBL-27086, Univ. of California, Berkeley, 1989.
[110]G. A. Christos, Preprint, Univ. of Western Australia, 1989.
[111]D. C. Bailey, Preprint, Univ. of Toronto, 1989.
[112]P. L. Hagelstein, Preprint, MIT, Cambridge, 1989.
[113]J. M. Carpenter, Nature (London) **338**, 711 (1989).
[114]M. Criber, M. Spiro, and J. Favier, Phys. Lett. B **228**, 163 (1989).
[115]L. Cranberg, Nature (London) **339**, 515 (1989).
[116]K. Gac, M. Kolonowski, Z. Skladanowski *et al.*, Preprint, Kaliski Institute of Plasma Physics, Warsaw, 1989.
[117]R. Pool, Science **244**, 1039 (1989).
[118]C. Joyce, New Scientist, No. 1671, 34 (1989).
[119]B. Levi, Phys. Today **42** (6), 17 (June 1989).
[120]T. Takeda and T. Takizuka, J. Phys. Soc. Jpn. **58**, 3073 (1989).
[121]S. A. Semiletov, R. V. Baranova, Yu. P. Khodyrev *et al.*, Kristallografiya **25**, 1162 (1980) [Sov. Phys. Crystallogr. **25**(6), 665 (1980)].
[122]J. S. Blakemore, *Solid State Physics*, Cambridge University Press, N. Y. (1985), 2nd Edition [Russ. transl., Metallurgiya, M., 1972].
[123]R. Fischer and H Neumann, *Field-Emission from Semiconductors*, Fortschr. Phys. **14**, 603, 1966 [Russ. transl., Nauka, M., 1971].
[124]V. S. Bushuev, V. B. Ginodman, L. N. Zherikhina *et al.*, Preprint No. 43, (In Russian), Physics Institute of the Academy of Sciences of the USSR, M., 1990.
[125]P. I. Golubnichiĭ, E. P. Koval'chuk, G. I. Merzon *et al.*, Preprint No. 99, (In Russian), Physics Institute of the Academy of Sciences of the USSR, M., 1990.
[126]P. Bem, I. Paseka, I. Pecina *et al.*, Preprint, Inst. of Nuclear Physics. Physics, Czechoslovakian Academy of Sciences, 1989 (submitted to Z. Phys. A).
[127]P. I. Golubnichiĭ, G. I. Merzon, A. D. Filonenko *et al.*, Preprint No. 109, (In Russian), Physics Institute of the Academy of Sciences of the USSR, M., 1990.
[128]J. D. Davies, G. J. Pyle, G. T. A. Squier *et al.*, Nuovo Cimento **103**, 155 (1990).
[129]S. E. Segre, S. Atzeni, S. Briguglio *et al.*, Europhys. Lett. **11**, 201 (1990).
[130]P. I. Golubnichiĭ, A. D. Filonenko, V. A. Tsarev *et al.*, Preprint No. 129, (In Russian), Physics Institute of the Academy of Sciences of the USSR, M., 1990.
[131]P. I. Golubnichiĭ, V. V. Kuzminov, G. I. Merzon *et al.*, Preprint No. 172, (In Russian), Physics Institute of the Academy of Sciences of the USSR, M., 1990.

Translated by M. E. Alferieff